Application of chitosan-based materials in surgical or postoperative hemostasis

Yuanliang Xia[1], Ruohan Yang[2], Hengyi Wang[1], Yuehong Li[1] and Changfeng Fu[1]*

[1]Department of Spine Surgery, The First Hospital of Jilin University, Changchun, China, [2]Cancer Center, The First Hospital of Jilin University, Changchun, China

Uncontrolled bleeding from trauma or surgery remains an important factor affecting the survival and prognosis of surgical patients. Failure to timeously stop bleeding will not only prolong the operative time but also threaten the patient's life. Timely hemostasis after bleeding has become the most concerned event for surgeons. At present, the most commonly used hemostasis methods in the operating room include ligation of blood vessels, electrocautery, and gauze compression to stop bleeding. However, These hemostatic methods do great harm to surrounding tissues while achieving hemostasis. Based on tissue engineering repair strategies, the use of natural polymer materials as hemostatic agents has achieved clinical success. Gelatin sponge and cellulose gauze have been used clinically with good results. However, gelatin sponges are very expensive and place enormous financial pressure on patients. Therefore, there is an urgent need for new hemostatic materials for surgical hemostasis. Chitosan is a natural polysaccharide with biocompatibility and biodegradability, which plays an important role in tissue engineering and regenerative medicine. Chitosan gauze has been proven to have good hemostatic effects. The positive charge on the surface of chitosan can adsorb red blood cells and platelets at the bleeding site to form platelet thrombosis. However, chitosan is not easily soluble in water and has poor adsorption, which makes it a weak local hemostatic agent. Therefore, it is important to improve chitosan-based hemostatic material such that it l has an excellent hemostatic effect. In this review, we introduce the physiological coagulation process and discuss the physicochemical properties of chitosan and its role in hemostasis. Furthermore, we discuss the advantages and disadvantages of chitosan-based hemostatic materials. Finally, we summarize and discuss chitosan-based hemostatic materials.

KEYWORDS

hemostasis, chitosan, biomaterial, gelatin sponge, platelets, red blood cells

1 Introduction

Rapid hemostasis is of great significance in cases of massive bleeding caused by surgery and trauma. Trauma is the fourth leading cause of death for patients under the age of 45, and 40% of deaths are due to bleeding (Herrold et al., 2021). Excessive bleeding disrupts hemodynamics, prolongs operative time, increases the risk of transfusion infection, and endangers the patient's life (Wang et al., 2019a; Eden et al., 2021). Administering anticoagulant therapy in the perioperative period to ensure smooth operation will also increase the risk of bleeding during or after the operation (Briete et al., 2022). In addition, people with hemophilia have poor blood clotting conditions and can bleed without trauma (Pai, 2021). Bleeding is a serious concern for both physicians and surgeons. Timely hemostasis to reduce bleeding can improve patient survival (Long et al., 2018). It is vital that surgeons are able to rapidly achieve hemostasis (Herrold et al., 2021).

At present, the commonly used hemostasis methods include tourniquet, compression, packing, electrocautery, and ligation of blood vessels in the operating room (Wang et al., 2019a). Tourniquet hemostasis is often used for distal hemostasis at trauma sites, during upper and lower limb surgery, etc. (Ajibade et al., 2021). A tourniquet compresses large blood vessels supplying the affected area to reduce blood flow to the area. A tourniquet can reduce the blood flow in the surgical area and shorten the operative time. However, tourniquet pain is the most common complication of tourniquet use (Kamath et al., 2021). Tourniquet usage time is proportional to postoperative tourniquet pain (Kamath et al., 2021). In addition, tourniquets block large blood vessels and seal the corresponding tissues and organs, resulting in insufficient blood flow supply to tissues and organs and potentially resulting in organ failure. Therefore, it is not recommended to use tourniquets for a long period of time. Ligation of blood vessels to stop bleeding is mainly used for bleeding that unintentionally damages blood vessels during surgery, where there is difficulty to clamp with hemostatic forceps; it has a better effect on large blood vessel bleeding (Paquette et al., 2018). Electrocautery burns wound tissue and blood vessels during tissue separation and cutting to control bleeding from small blood vessels (Merajikhah et al., 2022). Electrocautery is widely used clinically; however, it produces carcinogenic smoke particles (Watters et al., 2022). These fumes directly enter the respiratory tracts of doctors and nurses, causing
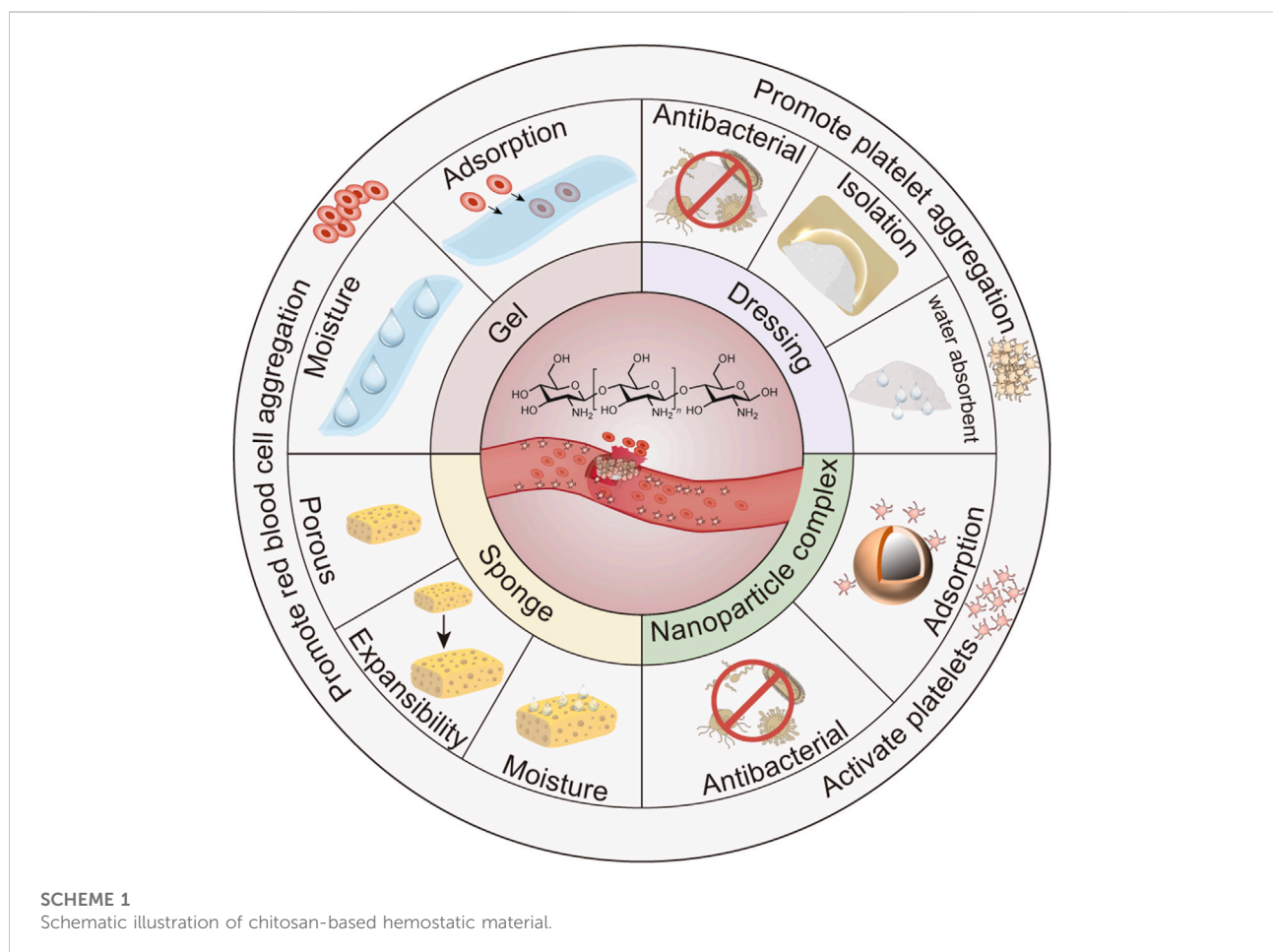

SCHEME 1
Schematic illustration of chitosan-based hemostatic material.

TABLE 1 Preparation method and hemostasis time of chitosan-based hemostatic material.

Hemostatic material	Composition	Preparation method	Hemostasis time *in situ*	Result	References
Gel	Self-assembling peptides	Self-assembling peptides were mixed with CMCS after 48 h of incubation at room temperature	15 ± 3 s	Self-assembled polypeptides can be combined with glutamate aminotransferase in blood and rapidly transformed into gels to achieve rapid hemostasis	Hao et al. (2020)
	HPCS, SPI	Mix HPCS powder with water and stir for more than 2 hours, then mix with SPI in a certain proportion, add Epichlorohydrin and stir for 30 min	75 ± 1.63 s	HCSH-30 stopped bleeding in 75 ± 1.63 s and improved hemostasis as compared with medical gauze	Zhao et al. (2020a)
	OHA, CMCS	CMCS and OHA were prepared in normal saline solution at the concentration of 3% wt. The two solutions were mixed by equal volume to form a hydrogel	38.9 ± 8.7 s	CMCS- OHA with good biodegradability and biosafety has good hemostatic and sealing ability, is a potential clinical hemostatic sealant	Xia et al. (2021)
	OSA,CMC,GEL	The OSA was mixed with an equal volume of CMC, GEL mixed solution in equal volume and stirred for 6 h. The reaction was terminated by the addition of ethylene glycol	62 s	Hydrogels can be rapidly formed *in situ* within 30 s and exhibit good adhesion strength	Cao et al. (2019)
	Zeolite, CS, Sodium alginate	Sodium alginate was mixed with zeolite and washed with deionized water after stirring with a magnetic stir bar at 300 rpm for 3 days	14.4 ± 0.31	Polymer hydrogel-aluminosilicate composite material may serve as a platform for an effective hemostatic agent that incorporates multiple mechanisms of action	Fathi et al. (2018)
	Chitosan, diatom, biosilica, DA	DB, chitosan, and DA mixture were added in sodium hy-droxide solution dropwise, and aerosols were made by solvent displacement	70 s	The strong interface effect between aerogel and blood is able to promote erythrocytes aggregation, platelets adhesion, and activation, as well as, activate the intrinsic coagulation pathway to accelerate blood coagulation	Li et al. (2020a)
	CMCS, PDA, PAM	DA was added to CMCS to polymerize for 10 min, and AM and initiator were added to form a gel. Lyophilized at −80℃ for 3 days	60 s	The hydrogel had multiple functionalities, such as tissue adhesive, biocompatible, self-healing, and antibacterial properties	Rao et al. (2022)
	HBC,CS,PDA	The CS was dissolved in acetic acid and the composite hydrogel was obtained after dialysis. The PDA was dispersed into a CS:HBC solution with a weight ratio of 1:3	19.67 s	The composite HCS-DOPA hydrogel has lower hemolysis rate and shorter clotting time	Zhang et al. (2019)
	HBC,CS,DOPA	Dissolve 0.38 g of HBCS in 20 ml of deionized water, add 3,4-dihydroxyphenylacetic acid and stir for 30 min. Lyophilized by dialysis after addition of CS.	30s	HBCS-C hydrogels possessed the properties of thermosensitivity, injectability, tissue-adhesion, biodegradation, biocompatibility, and wound hemostasis	Shou et al. (2020)
	PEG,CS,HA	CS-HA was dissolved into PBS with vigorous stirring for 4 h at room temperature, and after lyophilization, a double network hydrogel was formed with PEG at a molar ratio of 1:1	-	CS-PEG-HA promotes angiogenesis, collagen deposition and epidermal regeneration	Li et al. (2022)
凝胶	PEGSH, PEG	CS was dissolved in glacial acetic acid and polyethylene glycol terminated with sebacic acid. The 2-week solution was mixed for a polycondensation reaction	50 s	The hydrogel exhibited a shorter blood clotting time (50 s) and a lower coagulation index than the commercial chitosan sponge (288 s)	Song et al. (2021)
Dressing	CS, Aluminum chloride	The inorganic hemostatic agent was added to the acetic acid solution of CS and stirred magnetically. The solvent was then removed in a 48℃ oven	73 ± 9 s	The dressing has an irregular microporous structure that absorbs the maximum percentage of blood to form clots	Koumentakou et al. (2020)

(Continued on following page)

TABLE 1 (*Continued*) Preparation method and hemostasis time of chitosan-based hemostatic material.

Hemostatic material	Composition	Preparation method	Hemostasis time *in situ*	Result	References
	capric acid, OD,CS	CA was added to absolute ethanol, then added dropwise to CS solution and stirred for 24 h to obtain CSCA. The volume ratio of OD to CSCA was 1:2 and stirred for 2 minutes, and then freeze-dried	79 s	C-OD has high porosity (>78%) and swelling ratio, and the mean hemostasis time of C-OD is reduced compared to gelatin sponge	Wang et al. (2022)
	Carrageenan, CS	The citric acid solution of CS was mixed with the aqueous solution of carrageenan and stirred under a magnetic stirrer. After freeze-drying, a hemostatic dressing was obtained	-	The higher swelling, surface area and mesoporous structure of the composite dressing exhibits excellent hemostatic activity through higher blood cell and platelet adhesion	Biranje et al. (2020)
	Ag@MOF, Silk sericin, GO	AgNP solution and graphene oxide solution were mixed and stirred for 24 h, washed with alcohol and deionized water for 3 times, and then dried at 60°C for 24 h to obtain Ag@MOF-GO composites	-	The material has good biocompatibility and efficient coagulation function	Zhang et al. (2021)
	DAMA, Zinc-Silver Nanoparticles	Quaternary ammonium salt chitosan and zinc-silver nanoparticles were dissolved in deionized water, and DAMA was added and stirred to form a homogeneous liquid	129 ± 22 s	Hydrogel dressings have faster gelation, stronger tissue adhesion, excellent biocompatibility and hemocompatibility, good antibacterial properties and the ability to scavenge free radicals, which can effectively promote hemostasis and wound healing	Yang et al. (2022)
	PEG, Glyceryl Sebacate and Quaternary Amino Chitosan	EDC was used as dehydrating agent and DMAP was used as catalyst to synthesize glycerol sebacate, which was then mixed with quaternary amino chitosan	-	The self-healing antibacterial and antioxidant conductive hydrogel significantly enhanced the wound healing process in a full-thickness skin defect model	Zhao et al. (2017)
	CS, Calcium Alginate	CS was dissolved in acetic acid solution, alginate dressing was soaked in CS solution for 30 min, taken out and dried in an oven at 60°C for 30 min	-	CCAD is a better choice in wound care due to its antibacterial property, biocompatibility, moisture retention, healing promotion, and non-cytotoxicity characteristics	Zhao et al. (2020b)
海绵	PVA,CS	CS and PVA are dissolved in weak acid solution and foamed under acid catalysis. Finally, the newly synthesized PVA-CS sponge was compressed in one direction to form a micro-cylinder	10 s	PVA-CS30 sponge (30% by weight of CS) has good bacteriostatic and hemostatic effect without compromising the mechanical properties of PVA	Zhao et al. (2019)
	SIP,CS	CS was dissolved in acetic acid solution and SIP was dissolved in deionized water. 15 ml CS and 5 ml SIP were mixed and stirred. Form SIP-CS.	-	SIP-CS can adsorb blood cells and quickly stop bleeding, and can also promote wound healing, re-epithelialization and repair of epidermis and dermis	Huang et al. (2018)
	Cellulose, CS	3 g of cellulose was dissolved in urea aqueous solution, and 4 g of chitosan was added. After thorough mixing, add sodium lauryl sulfate and stir at high speed to form a rich foam	34 s	CS/Cel sponge has good biocompatibility and hemostatic ability, and is a promising candidate for rapid hemostasis under severe bleeding	Fan et al. (2020)
	Cellulose, CS	The foam was prepared in the same manner as above. The foam was added to an ethanol bath at -40°C for 10 min, and a porogen (Na_2SO_4) was added to the foam under high-speed mixing, and a new hemostatic sponge was obtained after freeze-drying	67 s	CS-Cel composite sponge has good water absorption and deformation recovery ability. Generally, it can be restored to its original state within 10 s	Fan et al. (2021)
	COL,CS,PAAS	Quaternary ammonium salt (QAS) chitosan modified with dihydroxy and oxadiazole groups, mixed with COL, sodium polyacrylate (PAAS) and lyophilized	50 s	PQC sponge exhibits efficient antibacterial and hemostatic properties, superior to chitosan medical sponges	Liu et al. (2021)

TABLE 1 (*Continued*) Preparation method and hemostasis time of chitosan-based hemostatic material.

Hemostatic material	Composition	Preparation method	Hemostasis time *in situ*	Result	References
	QAS-CS, SPI	Disperse 10 g of SPI powder into 60 g of distilled water and dissolve 6 g of QC powder into 94 g of alkaline NaOH solution. . The QC and SPI solutions were mechanically mixed to prepare a series of homogeneous SPI/QC mixtures, lyophilized	<50 s	SQS-50 performed best in reducing blood loss and time to hemostasis, overall hemostasis of SQS-50 was comparable to commercial gelatin sponges	Wang et al. (2021b)
	CS, gelatin sponge	Dissolve chitosan in 0.5 M vitamin C solution and gelatin (G) in demineralized water at 50 C. The two solutions were mixed and stirred at room temperature for 10 minutes and then freeze-dried	46.8 ± 3.1 s	CG is a potential biomaterial for surgical hemostasis to reduce bleeding with low pressure and absorbable properties	Lan et al. (2015)
	PEO, CS	Dissolve Ch (2 g) and PEO (3 g) in 100 ml of 50% acetic acid and stir at room temperature for 24 h. After electrospinning, the electrospun membranes were vacuum dried at room temperature for 12 h	80.6 ± 5.7 s	The porosity of ChEsM was significantly higher at 77 ± 3%, and ChEsM exhibited high biocompatibility and sufficient *in vitro* hemostatic blood interaction	Deineka et al. (2021)
Nanocomposites	CS, Ethanol	Chitosan was dissolved in ionic liquid 1-ethyl-3-methylimidazolium acetate (EMIM Ac) to form a solution, and then the chitosan/EMIM Ac solution was flow-injected into ethanol to form beads of uniform size. The formed chitosan beads were obtained after ethanol solvent exchange with water and freeze drying	-	Chitosan beads have high swelling ability and good biocompatibility. They are effective in inducing blood coagulation and coagulation and have potential use as hemostatic dressings for hemostasis in trauma	Li et al. (2020b)
	CaCO3, CS	Chitosan was dissolved in acetic acid solution, and CaCO3 powder was dispersed in 200 ml of distilled water and poured into 200 ml of chitosan solution. The CS-CaCO3 composites were obtained after freeze-drying	-	CS-CaCO 3 composite has shorter bleeding time and better wound healing properties	He et al. (2021)
	Calcium alginate, CS	CS was dissolved in acetic acid solution, added calcium alginate and magnetically stirred for 1 h. Washed with water and ethanol in turn, then dried under vacuum at 70°C	53 ± 10 s	CSMS@Alg microspheres showed much better *in vitro* and *in vivo* hemostatic efficacy than porous chitosan microspheres	Wu et al. (2020)
	Zinc alginat, CM	CS was dissolved in the acetic acid solution, then 4 ml of ZnCl 2 solution was added dropwise to the emulsion and stirred for an additional 1 h. The microspheres were washed several times with water and ethanol sequentially and dried in a vacuum oven at 50°C	55 s	CS@ZnAlg microspheres are biocompatible, biodegradable, and non-cytotoxic, making them a promising fast and safe hemostatic agent	Pan et al. (2018)
	CS, Dopamine, Silica	Add 2 g of CS to 100 ml of acetic acid solution, add 200 mg of dopamine and 200 mg of silica to the chitosan solution and stir well	-	CDDs are able to absorb water quickly and efficiently, thereby introducing aggregation and adsorption of blood cells	Wang et al. (2018)
	OB, CS, COL	Dissolve CS in acetic acid and disperse lyophilized OBC (0.1 g) and collagen powder (0.09 g) in 30 ml of deionized water at 4°C. Mixing and stirring two solutions to make nanocomposites	86 s	Sponges exhibit better antibacterial properties, biodegradability and biocompatibility	Yuan et al. (2020)
	MSP,CS	Microporous starch particles (MSP) were treated with sodium trimetaphosphate to form microporous structure, in which prothrombin was embedded to form chitosan microporous starch particles	50 s	The composite exhibits good biocompatibility and effective degradability, which can effectively control wound bleeding	Shi et al. (2020)

discomfort and disease. In addition, smoke blocks the surgical field of view and prolongs the operative time (Gioutsos et al., 2022). Antifibrinolytic drugs, such as tranexamic acid, can also be used for local hemostasis (Davis et al., 2021). However, the dosage of tranexamic acid, mode of administration, and dosing interval affect the hemostatic effect, and high doses of tranexamic acid can cause seizures in patients (Colomina et al., 2021). Therefore, there is an urgent need to develop new hemostasis methods to manage clinical bleeding.

Topical hemostatic agents, such as gelatin, cellulose, and dressings, have been developed for clinical local hemostasis (Roshkovan et al., 2021; Shah and da Cruz, 2021; Sokolakis et al., 2022). The hemostatic effect of these materials is better than that of traditional gauze, and there is no toxic effect on the surrounding tissue. However, gelatin sponges are also expensive. A small piece of gelatin sponge costs thousands of dollars, imposing a serious financial burden on patients. Chitosan (CS) is a natural polysaccharide. CS is biocompatible and biodegradable and plays an important role in tissue engineering and regenerative medicine, including anti-tumor, bracket, hemostasis, antibacterial, anti-inflammatory, vaccine and preservatives (Hafsa et al., 2021; Huerta-Madroñal et al., 2021; Li et al., 2021; Lin et al., 2021; Yadav et al., 2021; Yan et al., 2021; Yang et al., 2021). The positively charged groups of CS can attract to negative charges on red blood cells (RBC) and platelets at the wound site, thereby achieving hemostasis (Khan and Mujahid, 2019). Therefore, medical CS hemostatic materials have been produced in large quantities for clinical use (Benesch and Tengvall, 2002). However, low molecular weight CS has low solubility in water and cannot effectively interact with plasma components, and thus fails to achieve a hemostatic effect (Yang et al., 2008). In addition, once the water-insoluble CS enters the blood, it is transported to the small blood vessels and causes distant normal blood vessel embolism, resulting in unnecessary complications for patients and clinicians (Varshosaz, 2007). Therefore, many improved chitosan-based hemostatic materials have been designed for hemostasis (Scheme 1 and Table 1). In this review, we first introduce the process of physiological hemostasis and physicochemical properties of chitosan as a hemostatic material. Second, we discuss the application of chitosan-based materials in hemostasis. Finally, we discuss the application prospects of chitosan-based hemostatic materials.

2 Physiological hemostasis

The blood vessel wall is composed of a monolayer of endothelial cells that maintains a certain vascular tone and keeps the vascular intima smooth (Méndez-Barbero et al., 2021). Vascular endothelial cells use l-arginine to synthesize nitric oxide (NO) via NO synthase. NO shuttles freely in the blood and inhibits platelet adhesion and aggregation; therefore, neither aggregation nor leakage of blood components occurs in the blood (Neubauer and Zieger, 2022).

When endothelial cells are damaged, subendothelial smooth muscle leaks. Under the stimulation of local vasoactive substances, such as bradykinin, histamine, vasopressin, and vasoconstriction, the diameter of the tube is reduced, and the blood flow is lessened (Durand and Gutterman, 2013). The injured endothelium leaks von Willebrand factor (vWF) and collagen fibers, platelets roll along endothelial cells to subendothelial collagen fibers and vWF areas; Gp Ib-IX receptors, receptor glycoprotein VI (GPVI), and integrins on platelets α2β1 bind to intraendothelial vWF in a process called platelet adhesion (Sun et al., 2021; Bendas and Schlesinger, 2022). vWF is synthesized by macrophages and endothelial cells and stored in endothelial Weibel-Palade bodies (WPB) and platelet α-granules (Michels et al., 2022). vWF reacts rapidly in hemostasis and inflammation and is considered a marker of acute inflammation (Ruggeri and von Willebrand factor, 1997). Once the Gp Ib-IX receptor binds to vWF, ADP and thrombin activate the platelets. Activated platelets continue to activate other platelets through calcium-and phospholipase A2-mediated tyrosine kinase pathways, thromboxane A2 (TxA2), and thrombin-mediated G protein-coupled receptor pathways (Broos et al., 2011). Thrombin also stimulates platelet granules to release platelet-activating factor and adenosine diphosphate (ADP). When ADP is released, it binds to P2Y1 and P2Y12 receptors on the platelet membrane (Broos et al., 2011). P2Y1 induces pseudopodia shape changes and contributes to platelet aggregation, while P2Y12 plays a major role in inducing the coagulation cascade (Sirotkina et al., 2016). ADP binds to its receptor and induces the expression of the glycoprotein IIb/IIIa (Gp IIb/IIIa) complex on the platelet membrane surface. The Gp IIb/IIIa complex is a calcium-dependent collagen receptor that is required for platelet-endothelial cell adhesion and platelet-platelet aggregation (Sukhinina et al., 2022). Activated platelets synthesize TXA2, which further enhances vasoconstriction and platelet aggregation (Broos et al., 2011). After platelet aggregation, the Gp IIb/IIIa complex adheres to vWF and fibrinogen to form a platelet thrombus (Broos et al., 2011; Sukhinina et al., 2022). The process of platelet thrombus formation is called primary hemostasis.

After platelet hemostasis, coagulation factors activate fibrinogen to form fibrin via a cascade of actions. Fibrin interweaves into a network to form a more stable fibrin hemostasis, a process known as secondary hemostasis. Coagulation factors are mostly various protein components synthesized by the liver that are involved in the blood coagulation process. To date, 13 coagulation factors have been identified, namely coagulation factors I-VIII. The prothrombin complex formed by coagulation factors V and X is the key factor driving thrombin generation (Camire, 2021; Lam and Moosavi, 2022). Tissue factor (TF) is released when the blood vessel is damaged and collagen fibers in the subintima are exposed, which is initiated when TF binds to FVII, activates FVII to factor VIIa (FVIIa), and forms a TF-FVIIa complex (Batsuli and Kouides, 2021). Once factor X is activated to FXa by the TF-FVIIa
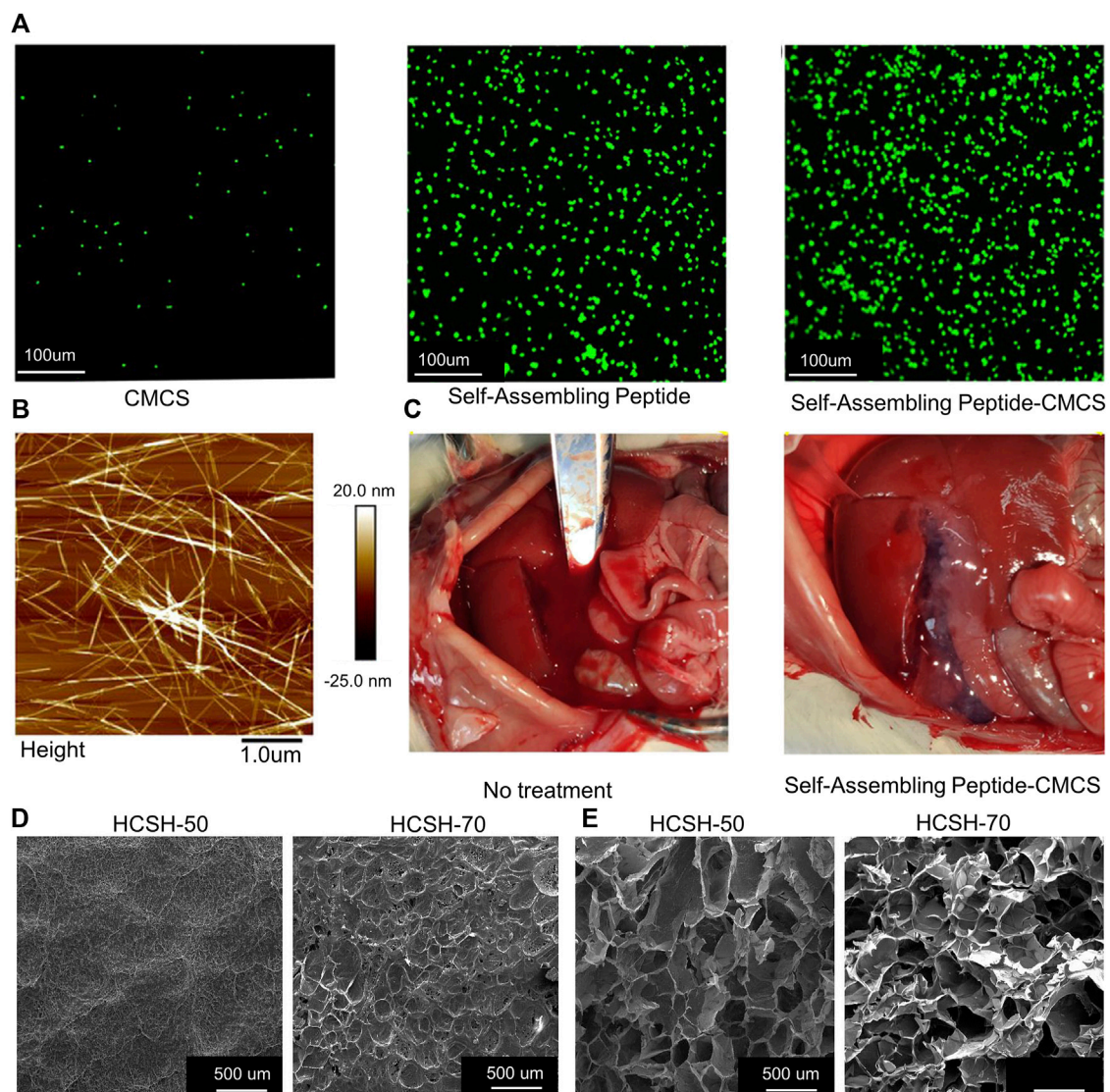
FIGURE 1
(A) Platelets were stained with Calcein-AM for fluorescence microscopy. Adsorption capacity of CMCS, self-assembling peptide, and self-assembling peptide-CMCS to platelets. **(B)** Structure of self-assembling peptide-CMCS under Atomic Force Microscopy. **(C)** Hemostasis of self-assembling peptide-CMCS and control rat models of liver injury. **(D)** Surface structure of HCSH-50 and HCSH-70. **(E)** HCSH-50 and HCSH-70 under scanning electron microscope. Reproduced with permission from (Zhao et al., 2020a; Hao et al., 2020).

complex, the cascade continues along a common pathway to convert fibrinogen to fibrin. Among them, TF is the initiation of the extrinsic coagulation pathway and FVII is the initiation of the intrinsic coagulation pathway (Batsuli and Kouides, 2021). FXa generated by the extrinsic and intrinsic coagulation pathways can form FXa-FVa-Ca2+-phospholipid complexes, namely, prothrombinase complexes, with FVa on the surface of phospholipid membranes in the presence of Ca2+. The prothrombin complex converts prothrombin (FII) to thrombin (FIIa). Thrombin hydrolyzes fibrinogen into fibrin monomers, which polymerizes fibrin monomers into fibrin in

the presence of calcium ions. Fibrin forms a local network to achieve hemostatic effects.

3 Chitosan

3.1 Physical and chemical properties of chitosan

CS is a natural polymer obtained by the deacetylation of chitin (Yadav et al., 2021). CS has a nitrogen content of 6.80% or

higher than that of chitin (Ardean et al., 2021). Therefore, CS has low viscosity, biocompatibility, and biodegradability (Othman et al., 2021). Unlike most natural polysaccharides, CS is a positively charged biopolymer because of the presence of amino groups in its backbone (Balan et al., 2021; Seidi et al., 2021). The physicochemical properties of CS are inversely affected by its molecular weight and degree of deacetylation (Croisier and Jérôme, 2013; Ardean et al., 2021). High-molecular-weight CS is 190–375 kDa, and low molecular weight CS is 20–190 kDa (Younes and Rinaudo, 2015; Azmana et al., 2021). When the degree of deacetylation (DDA) is >90%, CS is slightly cytotoxic and nondegradable (Caprifico et al., 2021). CS is broken down into glucosamine and N-acetylglucosamine components in the body (Bennett and Littlejohn, 2014). Therefore, understanding the physical and chemical properties of CS is of great significance for its improvement.

3.2 Chitosan hemostasis

Red blood cells are the main component of the blood, they transport oxygen in the blood, and maintain intravascular pressure. Both red blood cells and platelets have negatively charged surfaces, and because the surfaces repel each other, red blood cells run through the middle of blood vessels and platelets cling to the blood vessel walls (Khan and Mujahid, 2019). Owing to the smooth surface of the intima of the blood vessel, platelets cannot aggregate on the blood vessel wall. CS has no intrinsic hemostatic properties and acts independently of the coagulation system. CS exerts an excellent hemostatic effect even in patients with coagulopathy liver disease (Millner et al., 2010). The aggregation of RBC and platelets by CS may be due to the mutual attraction between the positive charges on the surface of chitosan and the negatively charged phosphatidylcholine and phosphatidylethanolamine on the surfaces of erythrocytes and platelets, resulting in the rapid aggregation of erythrocytes and platelets around the wound to achieve a hemostatic effect (Hu et al., 2018; Khan and Mujahid, 2019). In addition, a study found that CS can increase the expression of calcium ions and the GPIIb/IIIa complex in rabbits to promote the adhesion and aggregation of platelets (Chou et al., 2003). Different DDA and molecular weights cause different degrees of platelet aggregation. Studies have confirmed that DDA at 75–88% and high molecular weight (50–247 kDa) CS promote platelet aggregation (Khan and Mujahid, 2019). However, the more positive charges on the CS surface, the more conducive it is to hemostasis. However, excessive positive charges on the surface of CS inhibits blood coagulation (He et al., 2011). Therefore, it is important to improve CS to develop hemostatic materials suitable for clinical applications.

4 Chitosan-based materials for hemostasis

4.1 Hydrogels

Compared to traditional bandages or gauze, hydrogels keep wounds moist and prevent bacterial invasion (Rasool et al., 2019). CS gel can rapidly stop bleeding and reduce postoperative adhesions in Endoscopic sinus surgery (ESS) (Chung et al., 2016). However, CS is insoluble in water and is only soluble in weakly acidic environments, which limits its clinical application (Shariatinia, 2018). Adding carboxymethyl (-CH$_3$COOH) groups to the CS molecular chain can increase its water solubility (Shariatinia, 2018). Hao et al. used carboxymethyl CS (CMCS) to form hydrogels with self-assembled peptides (Hao et al., 2020). Self-assembled polypeptides can be combined with glutamate aminotransferase in the blood, which then rapidly transforms into gels to achieve rapid hemostasis. The mechanical strength of the gels mixed with different concentrations of O-CMCS and self-assembled peptides was different. The gel composed of 5.03 mg/ml self-assembled peptides and 0.44 mg/ml O-CMCS could achieve the maximum mechanical strength (3500Pa). *In vitro* experiments demonstrated that CMCS combined with self-assembling peptides increased platelet adhesion (Figure 1A). The self-assembled peptides combined with CMCS can form nanofiber-like structures (Figure 1B), which are beneficial for increasing the mechanical strength of the hydrogel. In the rat liver hemostasis model, the hydrogel can be observed to have obvious hemostatic effect (Figure 1C). However, as the concentration of CMCS increased, the hemostasis time was prolonged, which may have been caused by the inability of the high concentration of CMCS to mix uniformly with the blood (Hao et al., 2020). In another study, hydroxypropyl CS (HPCS) and soy protein isolate (SPI) formed hydrogels by crosslinking epichlorohydrin named as HCSH (Zhao et al., 2020a). The material preparation method is shown in Table 1. SPI has good biocompatibility and adhesion, which are favorable for hydrogel adsorption when combined with HPCS. The dense surface and internal porous structure of HCSH are favorable for platelet adsorption. Surface and SEM images of HCSH-50 (50% SPI in HCSH) and HCSH-70 (70% SPI in HCSH) are shown in Figures 1D,E. The higher the SPI ratio, the smaller the internal aperture. HCSH can effectively shorten the average hemostasis time and reduce bleeding in the rabbit liver. CMCS retains the free amino groups of CS and can adsorb platelets and RBCs (Jing and Fang, 2018). Hyaluronic acid (HA) regulates vascular wall permeability, promotes cell proliferation, and promotes wound healing (Aballay and Hermans, 2019). Xia et al. prepared a CMCS-oxidized HA hydrogel (CMCS-OHA) (Xia et al., 2021). The material preparation method is shown in Table 1. The pore diameter of the hydrogel ranges from 60 to 150 μm. The loose porous structure of the hydrogel is beneficial for trapping water

and nutrients and promoting cell adhesion. The hydrogel was excreted from the kidneys of mice, primarily through urine. Compared to sterile gauze, the lower IL-6 and TNF-α levels around the wound also indicated that the hydrogel had better wound repair ability. However, studies have shown that CMCS-OHA is more effective in promoting wound healing than hemostasis. Although hydrogels can promote wound healing, traditional hydrogels have poor tissue adhesion and cell affinity and cannot adhere to the wound, which is not conducive to hemostasis (Lee and Lin, 2022).

As an anionic polysaccharide, alginate exhibits a wide range of biomedical effects. Alginate is a cross-linking agent that can induce rapid cross-linking of hydrogels and nontoxic degradation *in vivo* (Balakrishnan et al., 2005). However, gels synthesized with alginate and CMCS do not have sufficient gel strength and adhesive strength; therefore, their hemostatic effect is not good (Cao et al., 2019). Cao et al. prepared injectable hydrogels utilizing *in situ* Schiff base bond formation between gelatin, CMCS, and oxidized sodium alginate (Cao et al., 2019). The material preparation method is shown in Table 1. The hydrogel exhibited an extremely fast *in situ* gelation rate (30 s) and an adhesive strength of 11 kPa. Since the increase of aldehyde groups accelerated the synthesis rate of Schiff bases, the gelation time was significantly shortened with the increase of the concentration of oxidized sodium alginate. However, when the oxidized sodium alginate concentration was too high, the solution became too viscous. Studies have shown that 15% sodium alginate can achieve the best results. Additionally, the addition of levofloxacin to the hydrogel could achieve local antibacterial effects. Studies have shown that hydrogels can release 54% of levofloxacin in 24 h with no toxicity to the surrounding cells. Compared with the control group, it reduced the bleeding time and blood loss by 84.2 and 82.2%, respectively, in rat liver injury. In addition to gelatin, zeolite has a very high water absorption rate and can quickly absorb blood cells and platelets at the damaged site to achieve hemostasis (Li et al., 2013). However, exothermic water and the reaction of the zeolite can damage the tissue and cells surrounding the wound. Peter et al. fabricated granular gels using zeolite, CS, and alginate (Fathi et al., 2018). The diameter of the zeolite affects the diameter of the granular gel, which in turn affects the hemostatic effect. Studies have shown that 1,693 ± 85 μm diameter particles can induce coagulation in 15 s, whereas 1,536 ± 96 μm diameter particles take 2 min.

Li et al. developed a CS/diatom-silica-based aerogel using dopamine as the cross-linking agent (Li et al., 2020a). The advantage of the gel is that it maintains the porosity of natural diatoms and provides the largest surface area (74.441 $m^2 g^{-1}$), allowing the blood to fully contact the diatoms, causing RBSs aggregation, platelet adhesion, and activation. Compared with a commercial hemostatic agent (Celox), the gel shortened the *in vitro* hemostasis time by 70 s. It also showed good hemostatic ability in rat tail vein

and femoral artery cutting models. In addition, polydopamine has good cell affinity and adhesion properties and is widely used in biomedicine (Barros et al., 2021). A fungal mushroom-derived CMCS-PDA hydrogel (FCMCS-PDA) was developed in a previous study (Rao et al., 2022). FCMCS also exhibited good antibacterial and procoagulant effects. Studies have shown that the maximum adhesion strength of the hydrogel to pig skin is approximately 29.6 ± 2.9 kPa, the tensile strain is 3,352% which is conducive to the adhesion of the hydrogel to the skin. The hydrogel with 0.4 wt% dopamine content had the best biocompatibility and achieved rapid coagulation within 60 s. However, this experiment did not measure the hemostatic effects of the hydrogel *in vivo*. Zhang et al. mixed CS with hydroxybutyl CS (HBCS) at a weight ratio of 1:3 to disperse dopamine in a CS-HBC solution to prepare temperature-responsive hydrogels (Zhang et al., 2019). The advantage of this gel is that it can achieve mutual transformation between sol and gel at physiological temperatures (between 4 and 37°C). Although the gel also has antibacterial properties, its hemostatic effects have not yet been evaluated.

The catechol group is the main adhesion group that enhances the adhesion of the tissue to the hydrogel through π-π stacking and hydrogen bonding interactions (Maier Greg et al., 2015). Attaching catechols to the chitosan backbone has excellent potential to increase the adhesion of CS hydrogels. Yin et al. designed and prepared catechol-hydroxybutyl CS (HBCS-C) by grafting hydroxybutyl and catechol groups onto a CS backbone (Shou et al., 2020). HBCS-C hydrogels have pore sizes ranging from 100 to 150 μm and the gel temperature is 32.1°C. The hydrogel can be firmly adsorbed on the wound surface via the interaction between the catechol groups, amino groups, and tissues. In addition, the gel exhibited excellent liquid-gel transition at different temperatures through changes in the hydrophilic-hydrophobic interaction and hydrogen bonding generated by the hydroxybutyl group. In a mouse model of liver hemorrhage, the gel was formed *in situ* within 30 s of the injection to prevent hemorrhage. A certain mechanical strength appears to be necessary for hemostasis of the skin surface (Wu et al., 2011). Polyethylene glycol (PEG) is a tunable macromolecular compound with multiple functional groups. Li et al. attached catechol-modified chitosan to PEG to form hydrogels with stronger mechanical properties (Li et al., 2022). The material preparation method is shown in Table 1. The multiple groups on PEG increase the adsorption capacity of the hydrogel, significantly enhance the compressive strength (50.81 kPa), and prevent liver hemorrhage in mouse models of liver hemorrhage. Most existing hemostatic materials are sponges or powders. These hemostatic materials are not easy to stretch and are not suitable for hemostasis of joints and limbs (Feng et al., 2020). Wang et al. encapsulated polyethylene glycol with 3-(3,4-dihydroxyphenyl) propionic acid-modified CS and p-hydroxybenzaldehyde (PEGSH) (Song et al., 2021). The hydrogel showed suitable stretchability (780%) and blood absorption (1,300% ± 50%) and the strong adhesion of hydrogel
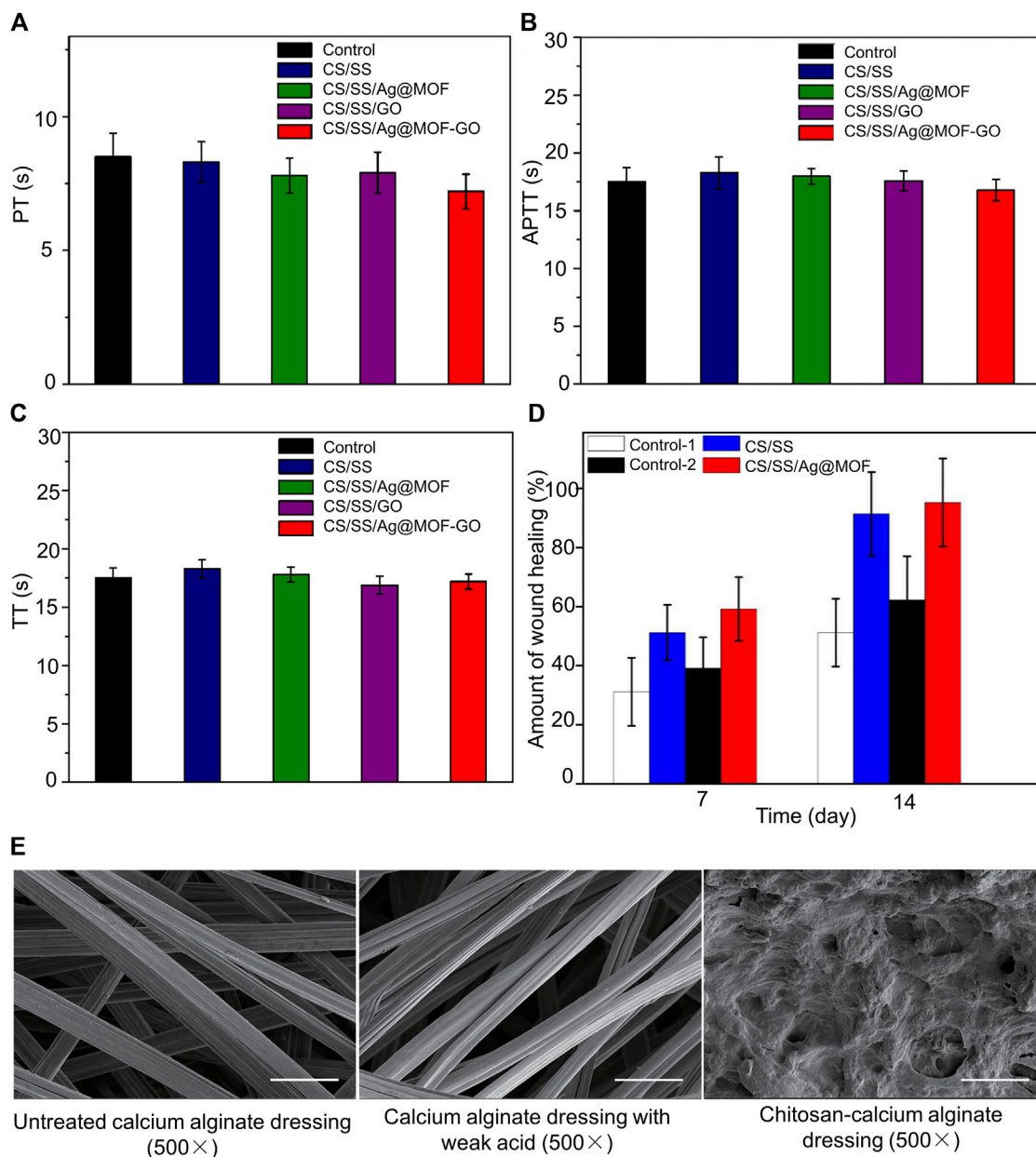
FIGURE 2
Assessment of the coagulation ability of the composite dressing showing the blood coagulation time PT **(A)**, APTT **(B)**, and TT **(C)** of rabbit blood in different groups. There was no significant difference in APTT, PT, and TT between different groups. **(D)** Wound healing rates between different groups on days 7 and 14. **(E)** Surface structure of calcium-free alginate, calcium alginate, and chitosan-calcium alginate dressings under scanning electron microscopy. Reproduced with permission from (Zhao et al., 2020b; Zhang et al., 2021).

is 68.5 kPa to ensure that the hydrogel can adhere to the wound. A stretchable hemostatic gel was formed by a reversible chemical bond between the amino groups of CS and benzoic acid. By adjusting the ratio of PEGSH, the chitosan hydrogel exhibited good stretchability and blood-blood adsorption. Moreover, the original shape could be restored at its highest stretch (81%) deformation.

4.2 Dressing

The ideal hemostatic dressing is permeable and highly absorbent in moist conditions, allowing for oxygen and fluid exchange, which are essential for wound protection (Wang et al., 2019b; Wang et al., 2021a). CS dressings have procoagulant and antibacterial properties compared with ordinary gauze (Wang

et al., 2021a). In a pig femoral artery hemostasis experiment, it was confirmed that the CS dressing has a porous structure, which greatly reduces the amount of femoral artery bleeding compared to traditional gauze (Wang et al., 2019c). However, the limited adhesiveness and water absorption of CS dressings limits their application to some extent.

Ioanna et al. added an inorganic hemostatic agent, aluminum chloride, to CS dressings to improve their hemostatic effect (Koumentakou et al., 2020). The best swelling ability of CS dressings which reached up to ~2,600 ± 560. Aluminum chloride achieves hemostasis by constricting the blood vessels and absorbing the surrounding water. It is a commonly used inorganic hemostatic agent (Howe and Cherpelis, 2013). Aluminum chloride and CS molecules form an ionically cross-linked network, making them fully in contact with blood to induce red blood cell and platelet aggregation. Although the dressing has been shown to shorten the clotting time *in vitro*, the disadvantage is that the dressing causes 5% hemolysis. Not only that, inorganic substances, such as residues in the body and low controllability (Granville-Chapman et al., 2011). Wang et al. grafted capric acid (CA) onto CS to form CSCA, which produced hemostatic sponges (C-ODs) via Schiff's base reaction with varying degrees of oxidized destrans (ODs) (Wang et al., 2022). ODs also exhibit tissue adsorption and hemostatic properties; however, excess ODs are cytotoxic (Elçin et al., 2020). ODs have a pore size of 100–200 μm and tissue adhesion of 4.74 kPa. The advantage of this dressing is that the degree of pre-freezing and the increased degree of cross-linking during preparation delay the formation of crystals within the material, resulting in a unique void content (>78%). This unique void ratio facilitates the dressing to absorb water and accumulate a large number of blood cells and coagulation factors in a short time. At the same time, the dressing also reduces the leakage of excess aldehyde groups in ODs and the cytotoxicity of the dressing. Compared with the clinically applied gelatin sponge, the hemostasis time of the C-ODs was reduced by 42%. However, crosslinking agents affect the polymer strength at different temperatures and concentrations (Ren et al., 2021). Carrageenan is an anionic sulfated polysaccharide used for stabilizing and thickening (Kalsoom Khan et al., 2017). However, carrageenan products are limited by their poor mechanical properties. CS and carrageenan were made into hemostatic dressings by ion complexation and freeze-drying by Santosh et al. (Biranje et al., 2020). The advantage of this dressing is that the negative effects of the cross-linking agents are avoided. The total surface area the dressing were 60.4 ± 0.2 m2/g and the average pore diameter was 4.5 ± 0.1 nm. The porous structure of the dressing can accelerate the wound healing process by promoting cell adhesion and proliferation at the wound site, absorption of exudates, and penetration of nutrients and oxygen. However, different ratios of CS and carrageenan had different effects on the degree of crystallization of the dressings. CS concentrations above 0.5%

(w/v) resulted in highly viscous and gelled solutions, whereas carrageenan concentrations above 0.5% (w/v) resulted in clumping.

Although CS dressings have certain antibacterial properties, their hemostatic effect on infected wounds requires further improvement. Zhang et al. combined a CS/sericin hydrogel (CS/SS) with a silver-graphene nanometal framework (Ag@MOF-GO) using the freeze–thaw cycle method (Zhang et al., 2021). The advantage of the dressing is that the amino carboxyl and hydroxyl groups in sericin can increase the adhesiveness and antibacterial and antioxidant properties of the dressing (Chouhan and Mandal, 2020). Ag@MOF-GO can achieve a slow release of Ag ions without causing the dressing to collapse. The dressing has a dense structure and a large surface area, which is conducive to the adhesion of platelets and red blood cells and accelerates blood coagulation. In the *in vitro* experiments, it was observed that the hemostasis time of CS/SS was close to 219 s, and the time of CS/SS/Ag@MOF-GO was not more than 160 s. However, in the process of *in vitro* coagulation experiments detected by rabbit blood, we found that in all experimental groups the activated partial thromboplastin time (APTT) was between 16.8 and 18.3 s, prothrombin time (PT) was between 7.2 and 8.5 s, and thromboplastin time (TT) was between 16.2 and 18.4 s (Figures 2A–C); indicating that CS/SS/Ag@MOF-GO does not enhance the release of coagulation factors. Moreover, CS/SS/Ag@MOF-GO also promoted wound healing (Figure 2D). This healing property is thought to be related to the antibacterial properties of the CS/SS/Ag@MOF–GO. Yang et al. composited methacrylate anhydride dopamine (DAMA) and zinc silver nanoparticles into CS to obtain a multifunctional CS dressing (Yang et al., 2022). The material preparation method is shown in Table 1. Among them, quaternary ammonium salt-improved CS and nanosilver can improve their antibacterial properties (Liang et al., 2020). Dopamine can increase tissue adhesion and antioxidant effects through surface interactions and hydrogen bonds, eliminating a large number of free radicals around infected wounds. The highest bond strength of the hydrogel is 0.052 ± 0.009 MPa. In addition, DAMA and zinc-silver nanoparticles formed a covalently cross-linked network *in vivo* to enhance the compressive strength of the dressing while providing an environment for calcium ions to participate in exogenous and exogenous hemostasis pathways. The dressing exhibited unique antibacterial and hemostatic advantages compared to no zinc-silver nanoparticles; however, too many nanoparticles (>2 wt%) made the CS dressing brittle. It would be better to replace zinc-silver nanoparticles with another antibacterial material that can improve the compressive strength of the dressing. Zhao et al. connected polyaniline to the CS skeleton and then mixed PEG, glycerol sebacate, and quaternary amino CS to create a hydrogel dressing with higher compressive strength and conductive activity (Zhao et al., 2017). The advantage of the dressing is that connecting polyaniline to the CS skeleton not only increases

the water solubility of CS but also endows CS with the ability to scavenge free radicals (Zhao et al., 2015). The amino and quaternary amino groups in this dressing impart electrical conductivity to the hydrogel with a maximum conductivity of 3.5 mS/cm at 25 °C. *In vitro* studies confirmed that the dressing did not destroy red blood cells and reduced the blood loss around the wound. In addition, dressing upregulates major growth factors, such as vascular endothelial growth factor and transforming growth factor beta (TGF-β), which are involved in the wound healing process, compared to commercial dressings. The calcium alginate-chitosan dressing developed by Zhao et al. can also be antibacterial and hemostatic (Zhao et al., 2020b). The surfaces of calcium-free alginate, calcium alginate, and CS-calcium alginate dressings are shown in Figure 2E. The CS-calcium alginate dressing has a rougher surface, which is more conducive to platelet adsorption. The advantage of this dressing is that it can absorb more than 20 times its volume of water and exchange calcium ions around the wound. As coagulation factors, calcium ions can accelerate the coagulation process.

4.3 Sponge

CS dressings and gels are often ineffective (Zhao et al., 2019). The advantage of the hemostatic sponge is its high blood-absorption rate. Materials with high water absorption can absorb a large amount of wound exudate, concentrate blood cells, and accelerate coagulation, thereby achieving rapid hemostasis (Okuda-Tanino et al., 2017). Polyvinyl alcohol (PVA) is a non-toxic water-soluble polymer. A PVA sponge causes physical hemostasis under local compression. Zhao et al. used CS and PVA crosslinked into a uniform material via a homogeneous foaming reaction (Zhao et al., 2019). The advantages of PVA-CS are its robust mechanical strength, rapid water-triggered swelling, and fast absorption speed. PVA-CS rapidly absorbs the blood around the wound and creates pressure on the surrounding blood vessels to prevent active bleeding. The huge spongy structure provided an adsorption surface for a sufficient number of platelets to attach and effectively inhibited femoral artery hemorrhage in rats within 10 s. However, studies have shown that excessive positive charges on the surface of CS have an inhibitory effect on blood coagulation (He et al., 2011). Squid ink polysaccharide (SIP) is a polymer extracted from squid ink, which has been found to activate coagulation factor FXII and has a good hemostatic effect (Kandra et al., 2012). Huang et al. prepared a CS hemostatic sponge by lyophilizing SIP and CS (Huang et al., 2018). The material preparation method is shown in Table 1. The advantage of this hemostatic sponge is that it can reduce the positive charge on the surface of CS and activate a coagulation cascade. However, reducing the positive charge on the surface of CS seems to be detrimental to the adsorption of RBC and

platelets. However, the massive pore structure of SIP-CS provides an attachment surface for blood cells and platelets. In the rabbit femoral artery hemorrhage model, the hemostasis time of the SIP-CS group was shortened by 54.67% compared with that of the CS group.

Cellulose with a high water absorption capacity can quickly absorb the blood around the wound, promote thrombosis, and achieve hemostasis (Behrens et al., 2014). The addition of a pore-forming agent to cellulose can increase its water absorption capacity. Fan et al. mixed cellulose and CS solutions and added a pore-forming agent to create a hemostatic sponge with abundant voids and strong water absorption (Fan et al., 2020). The introduction of CS can improve the compressive and antibacterial strengths of cellulose. However, the CS to cellulose ratio at different doses affected the properties of the hemostatic sponge. The higher the chitosan content, the lower the porosity of the hemostatic sponge, and the higher the compressive strength. When the ratio of CS to cellulose is 1:1, the compressive strength is 24.2 kPa and the porosity is 85.6%. A study of *in vitro* blood coagulation time found that when the ratio of CS to cellulose was 1:1, the whole blood coagulation time was the lowest (35 s). The hemostatic time in the rat liver injury model was 20 s. Another advantage of a hemostatic sponge is that it returns to its original shape within 10 s after being compressed or absorbing water. However, an excess of pore former can cause uneven dispersion of cellulose. In another study by Fan et al., adding surfactants to cellulose solutions increased the porosity and bulk (Fan et al., 2021). The hemostatic sponge fully recovers its shape within 5 s of compression and absorbs approximately 10–34 times its own weight in water. The hemostatic sponge in the rat leg artery hemostasis time (105 s) was significantly shorter than that of the commercially available gelatin sponge (372 s). However, surfactants reduce the compressive strength of hemostatic sponges.

Collagen has good biocompatibility and adhesion, can induce platelet aggregation, and can be applied to hemostatic materials (Okuda-Tanino et al., 2017). Compared to mammalian collagen, marine collagen (MC) has lower immunity and more stable physicochemical properties, attracting increasing attention (Lim et al., 2019). Chen et al. prepared CMCS-MC sponges by mixing CMCS and MC in a 6:1 ratio through freeze-thaw cycles and freeze-drying (Liu et al., 2021). The CMCS-MC hemostatic sponge has a highly porous microstructure (porosity ≈90%) with moderate compressive modulus (≈0.3 MPa), tensile strength (0.004 MPa) and high swelling ratio (≈3,500%). Compared with traditional gauze, CMCS-MC can shorten bleeding time and volume. Wang et al. developed a hemostatic sponge (SQS) using freeze-drying technology with SPI and quaternized chitosan (QC) (Wang et al., 2021b). The material preparation method is shown in Table 1. The surface morphology of SQS obtained using different weight ratios of QC differs (SQS-50 indicates that the weight ratio of QC is 50%). The SQS morphologies of the upper surface and cross section with
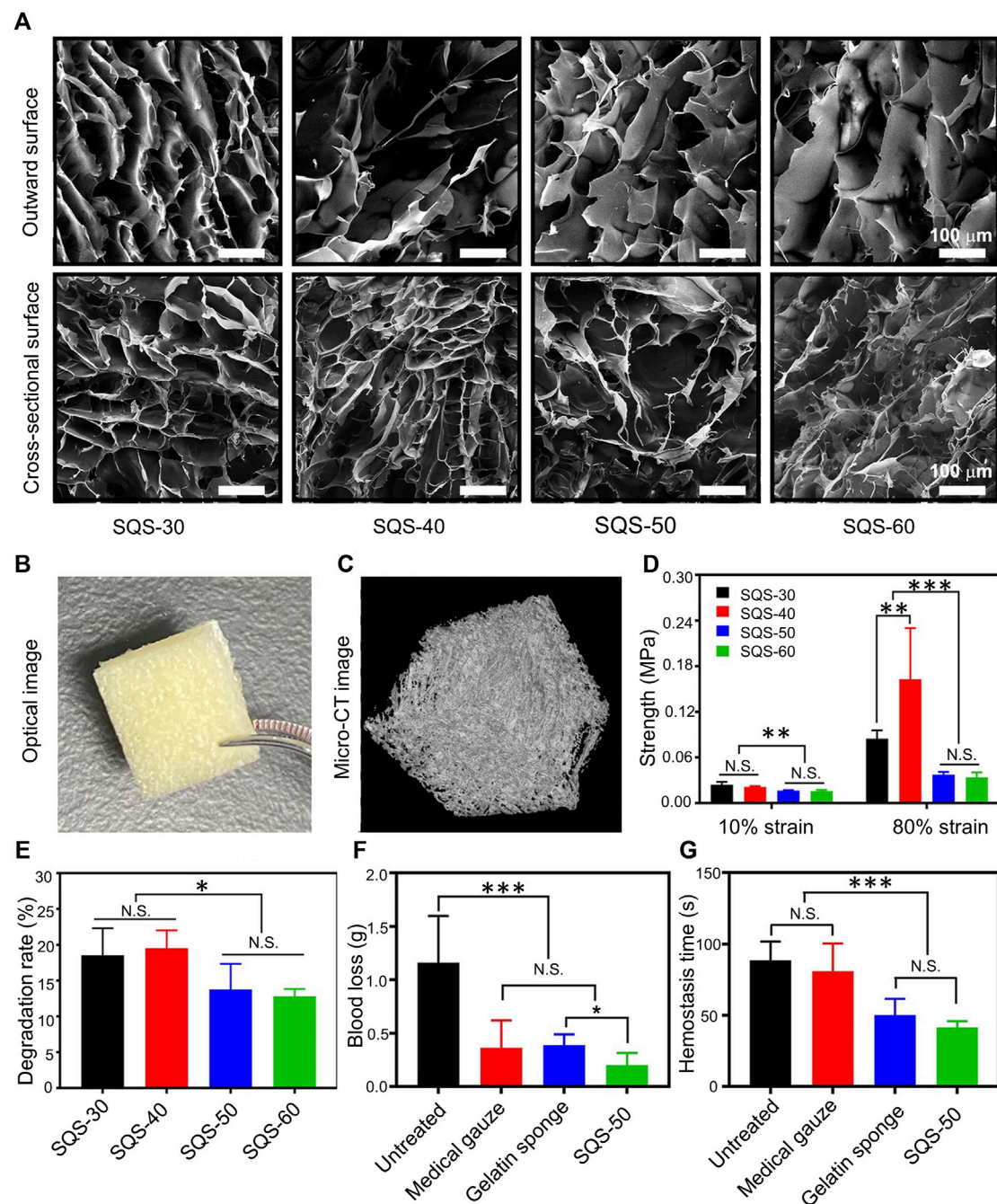
FIGURE 3
(A) Morphology of the upper surface and cross-section of SQS-30, 40, 50, and 60 (scale bar = 100 μm). **(B)** Optical images of SQS-50. **(C)** Micro-CT images of SQS-50. D) Results of the compressive strength at 10 and 80% SQS-30, 40, 50, and 60. **(E)** *In vitro* degradation experiments. Degradation rates of SQS-30, 40, 50, and 60 incubated with simulated gastric juice for 8 h at 37 °C with constant stirring. **(F)** Blood loss in a rat model of hepatic hemorrhage. **(G)** Hemostasis time in a rat model of hepatic hemorrhage. Reproduced with permission from (Wang et al., 2021b).

different QC ratios are shown in Figure 3A. As the QC content increased, the surface of the SQS became rougher and the pore size became larger. The compressive strength of SQS-50 is 0.037 ± 0.003 MPa. SQS-50 is shown in Figure B and C. The

porosity of the SQS hemostatic sponge can promote plasma absorption in a short time and activate red blood cells and coagulation factors, thereby enhancing blood coagulation. The hemostatic sponge had the highest mechanical strength at 80%

compression (Figure 3D). *In vitro* degradation experiments showed that the higher the QC content, the faster the degradation (Figure 3E). In the rat liver hemorrhage model, SQS reduced blood loss and hemostasis time (Figures 3F,G).

Gelatin is obtained during the degradation of the triple helical structure of collagen into single molecules. Gelatin has low antigenicity, good biocompatibility, and degradability and can activate platelets. It has been clinically used as a hemostatic material (Malda et al., 2003). The combination of CS and gelatin enhances the stability of gelatin. Wu et al. mixed CS with gelatin and used tannic acid as a cross-linking agent to prepare a hemostatic sponge using a gradual-based extraction and freeze-drying method (Lan et al., 2015). The advantage of this hemostatic gel is that it has a more stable structure and more uniform pore size than CS or gelatin sponge alone. The study confirmed that hemostatic sponges mixed with different proportions of CS and gelatin had different hemostatic effects, and the hemostatic sponges with a ratio of 1:1 mixed with CS and gelatin had the best hemostatic effect. Although gelatin has a good hemostatic effect, it is expensive.

The pore size of the hemostatic sponge could be increased by mixing the polymer and CS. However, the hemostatic sponge prepared in this manner was inferior to that prepared using the electrospinning technique. Electrospinning technology can be widely used in bioengineering and tissue engineering to synthesize three-dimensional porous materials from polymers. Electrospun CS enables the formation of CS sponges with high clot-forming activity and biocompatibility (Ding et al., 2019). However, the leaked hydrogen bonds of CS in acidic solutions cause great difficulties in the electrospinning process. Maksym et al. mixed polyethylene oxide (PEO) with CS (3:1) and dissolved it in an acetic acid solution (Deineka et al., 2021). PEO has good biocompatibility and can synthesize polymers in water (Zanchetta et al., 2020). The advantage of the electroviscosity sponge is that it can act as a hemostatic sponge with higher porosity (average pore area is 164 μm^2), which can accelerate the absorption of fluid around the wound. Compared to CS sponges, electrospun hemostatic sponges can improve blood adsorption. Nonetheless, there was no significant difference in the hemostasis time of electrospun sponges in rats compared to that of CS sponges.

4.4 Nanocomposites

The advantage of nanocomposites over dressings and sponges is that local hemostasis can be achieved regardless of wound shape. Nanocomposites can be locally absorbed without affecting surrounding tissue. Li et al. flowed a CS solution into an ethanol solution to form CS beads of uniform size after freeze-drying (Li et al., 2020b). The advantage of CS beads is that they have a high swelling ability and can absorb 30 times their weight in liquid. CS beads showed excellent cytocompatibility. However,

higher doses of CS beads (2–5 mg) did not accelerate blood clotting. Therefore, the application of CS beads alone did not achieve hemostasis. Calcium itself, as a coagulation factor, activates the coagulation cascade and accelerates fibrinogen formation. He et al. precipitated and mixed calcium carbonate on CS by wet granulation, which improved the hemostatic activity of the composites (He et al., 2021). The material preparation method is shown in Table 1. The particle radius of CS-CaCO$_3$ was approximately 600 nm, and the local release of calcium ions in the wound promoted platelet aggregation and activation and greatly shortened the coagulation time. Wu et al. prepared core-shell hemostatic particles using calcium alginate and CS (Wu et al., 2020). The density, porosity and water absorption of hemostatic particles are 0.1394 ± 0.012 g/cm^3, $93.2 \pm 4.3\%$ and 12.1 ± 1.7 g/g. The advantage of using CS as the core structure and alginate as the shell structure is that the core-shell structure significantly increases the contact area and improves hemostatic efficiency. In the rat liver tear model, the hemostasis time was significantly shortened to 53 ± 10 s. Although calcium ions can activate the coagulation response, the concentration of zinc ions in the blood is higher than that of calcium ions (Vu et al., 2013). Meng et al. introduced zinc ions in the form of zinc alginate into CS microspheres to form porous microspheres (Pan et al., 2018). The blood-absorbing microspheres have a porosity of 52.1% and a surface area of 48.9 m^2/g. The advantage of microspheres is that the addition of zinc ions can accelerate platelet aggregation and activation. At the same time, the strong water absorption of alginate also improved the water absorption capacity of CS hemostatic microspheres (1850%). Compared with CMCS (118 s), the *in vitro* whole blood clotting time of CS microspheres also significantly shortened the whole blood clotting time (55 s). Hemostatic microspheres can also act as a physical barrier to accelerate blood coagulation. However, alginate may cause hemolysis (Slowing et al., 2009).

Diatom biosilica (DB) negatively charged surfaces can significantly promote intrinsic coagulation by activating coagulation factors XI and XII and prekallikrein, resulting in effective hemostasis (Feng et al., 2016). Wang et al. prepared CS/dopamine/DB microspheres via alkaline precipitation (Wang et al., 2018). Encapsulating DB inside the microspheres protected its porous structure, and dopamine acted as a cross-linking agent to tightly bind CS to DB. The advantage of this microsphere is that its expansion rate (480%) is more than twice that of CS (220%). The hemolysis rate of microsphere is less than 5%, and the cell viability is above 80%. Studies have shown that CS gels can reach swelling equilibrium in water after 12 h (Bi et al., 2017), whereas CDDS can reach swelling equilibrium in water after 20 s. Another advantage of the microspheres is that alginate is encapsulated inside the microspheres, which reduces the hemolysis of alginate. The *in vitro* coagulation time proved that the CDDS coagulation time (1.35 min) was significantly shorter than that of CS (4 min).
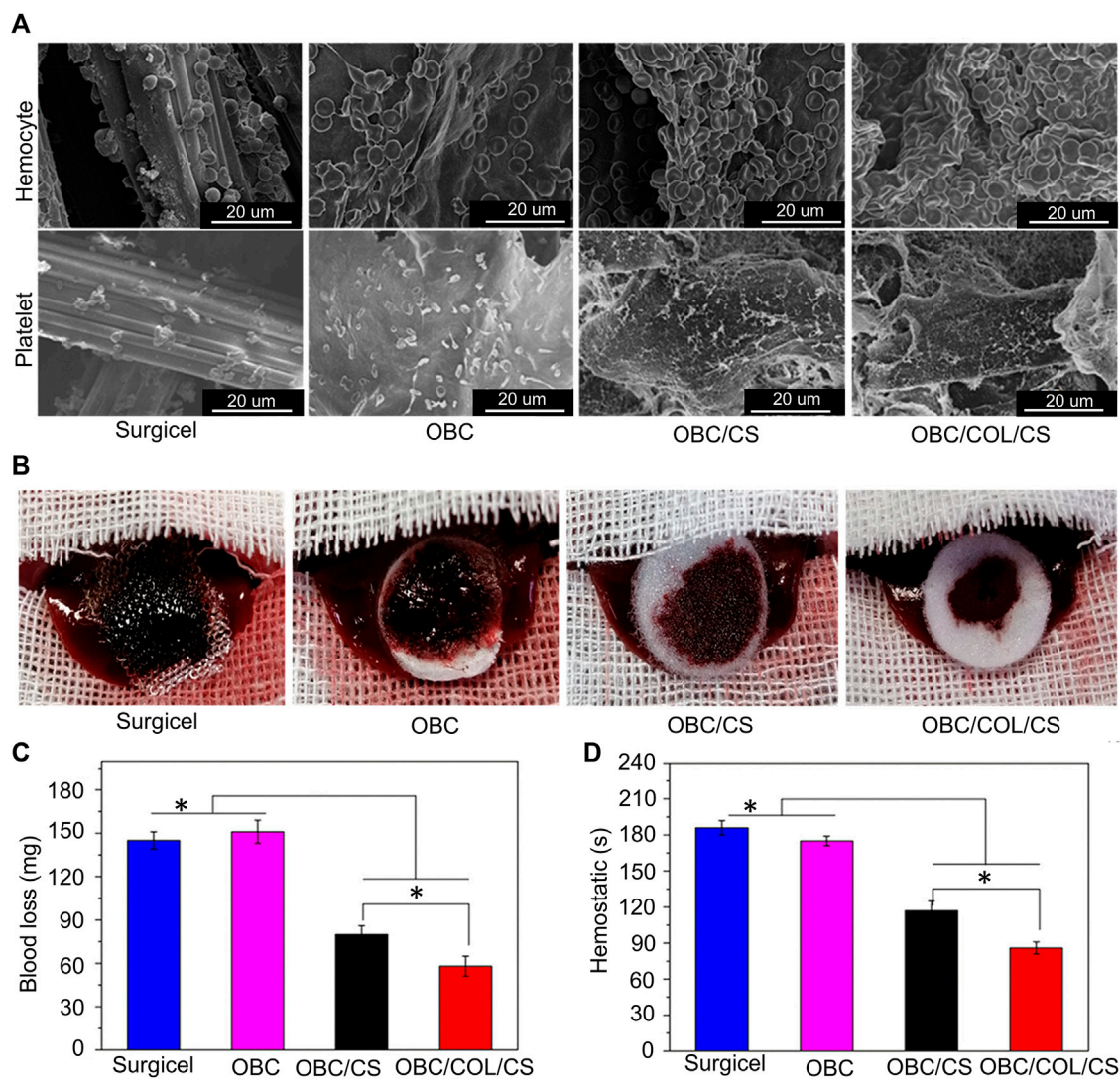
FIGURE 4
(A) SEM image of red blood cells and platelets adhering to the sample. **(B)** *In vivo* evaluation of the hemostatic capacity of the different complexes in a rat liver trauma model. **(C)** blood loss of the different complexes in a rat liver trauma model. **(D)** Time to hemostasis of the different complexes in a rat liver trauma model. Reproduced with permission from (Yuan et al., 2020).

Oxidized regenerated cellulose (ORC) is the most widely used absorbable topical hemostatic agent, which can be absorbed *in situ* after topical application with no toxic side effects on surrounding tissues (Blair et al., 1988). However, ORC locally leads to an increase in the carboxylic acid group content, which promotes the growth of bacteria that prefer acidic conditions and is not conducive to wound healing (Tefik et al., 2012). Bacterial nanocellulose (BNC) has a fibrous nanonetwork structure and good biocompatibility. Hong et al. developed ORC and BNC into oxidized bacterial nanocellulose (OBC) and converted CS, collagen, and OBC into an OBC/COL/CS composite (Yuan et al., 2020). The advantage of this composite material is that CS and collagen wrap around the ORC, which compensates for

the acidic condition of the ORC formed *in situ* and hinders the proliferation of bacteria. Simultaneously, the water absorption and swelling properties (166% swelling after 15 min) of the composite materials were retained. *In vitro* coagulation experiments showed that the composite material exhibited a strong coagulation ability within 10 s, twice as fast as the OBC group. *In vivo* experiments showed that the interconnected porous structure and high expansion rate of the composites enhanced the adsorption capacity of erythrocytes and platelets (Figure 4A). *In vivo* evaluation of the hemostatic ability of different complexes in a rat liver trauma model is shown in Figure 4B, which shows that the OBC/COL/CS composite had the best hemostatic effect with less blood loss (Figure 4C) and the

lowest hemostasis time (Figure 4D). The abundant hydroxyl and carbonyl groups in konjac gluco mannan molecules result in good water absorption (Chen et al., 2018). Shi et al. treated microporous starch particles with sodium trimetaphosphate to form a microporous structure and embedded prothrombin into it to form CS microporous starch particles (Shi et al., 2020). The material preparation method is shown in Table 1. The advantage of the hemostatic material is that the surface of the CS starch granules are rough and the interior is smooth and rich in a microporous structure. The porosity of hemostatic material is kept above 86%. When blood passes through microporous particles, it cannot stay at the junction between particles and blood because of its smooth internal structure. As blood passes through the granules, large amounts of thrombin attached to the interior of the granules activate fibrinogen into a fibrin network that captures the encapsulated blood cells and platelets to form thrombi.

5 Future perspective and conclusion

Uncontrolled bleeding is an important reason that affects the recovery and life of patients after surgery. At present, the commonly used hemostatic materials such as gauze and gelatin sponge have good hemostatic effect. However, gelatin sponges are expensive and often impose a heavy financial burden on patients. Therefore, it is very important to develop new hemostatic materials. Biomaterials have been widely used in tissue engineering. The advantages of natural biomaterials have been reported in various disciplines. In this review, we explore the applications of CS-based hemostatic materials. Although the CS material itself has a certain hemostatic effect, its shortcomings of low water solubility and poor adsorption limit the clinical application of CS hemostatic material. Poor water solubility will also cause CS to form a thrombus in the blood, which will cause harm to patients as blood flows to important organs, such as the heart and lungs. Therefore, this study summarizes the methods for improving the CS hemostatic material to increase its water absorption, porosity, and compressive strength of the hemostatic material. The porous surface facilitates the full contact of blood with the material and increases the aggregation of red blood cells and platelets. CS hydrogels have moisturizing effects and prevent bacterial invasion. The swelling and water absorption of the CS sponge effectively controlled local bleeding. These improvements have greatly improved the use of CS as a hemostatic material. However, the properties and effects of hemostatic materials obtained with different ratios of materials and CS differ. Moreover, research regarding these materials is limited to *in vitro* experiments and mammalian bodies and has not yet been widely used in clinical practice.

Nevertheless, both *in vivo* and animal experiments have confirmed that CS-based hemostatic materials have better hemostatic effects and reduce bleeding more effectively than cellulose gauze and gelatin sponge, which are commonly used in clinical practice. In addition,CS-based hemostatic materials mainly target RBS and platelets during physiological hemostasis. Future research can strengthen the study of CS-based hemostatic materials to enhance the coagulation pathway to form more stable hemostatic agents. More importantly, compared with gelatin sponge, the research and design of CS-based hemostatic materials are cheaper and greatly reduce the economic burden of patients. Therefore, CS-based hemostatic materials have great clinical potential, will be clinically applied in the near future, and can greatly improve the survival rate of patients with bleeding.

Author contributions

All authors read and approved the final manuscript. YL wrote the initial manuscript. CF and RH contributed new ideas. HY created the figures. YH and HY created Table 1. YL, HY, and YH revised the manuscript and approved the final version.

Funding

Acknowledgments

Conflict of interest

The authors declare that the research was conducted in the absence of any commercial or financial relationships that could be construed as a potential conflict of interest.

Publisher's note

All claims expressed in this article are solely those of the authors and do not necessarily represent those of their affiliated organizations, or those of the publisher, the editors and the reviewers. Any product that may be evaluated in this article, or claim that may be made by its manufacturer, is not guaranteed or endorsed by the publisher.

References

Aballay, A., and Hermans, M. H. E. (2019). Neodermis formation in full thickness wounds using an esterified hyaluronic acid matrix. *J. Burn Care & Res.* 40, 585–589. doi:10.1093/jbcr/irz057

Ajibade, A., Oladipo, O. M., Lawal, Y. Z., and Oluwadiya, K. S. (2021). A survey of the use of tourniquet among orthopaedic surgeons in Nigeria. *Niger. Postgrad. Med. J.* 28, 133–138. doi:10.4103/npmj.npmj_472_21

Ardean, C., Davidescu, C. M., Nemeş, N. S., Negrea, A., Ciopec, M., Duteanu, N., et al. (2021). Factors influencing the antibacterial activity of chitosan and chitosan modified by functionalization. *Int. J. Mol. Sci.* 22, 7449. doi:10.3390/ijms22147449

Azmana, M., Mahmood, S., Hilles, A. R., Rahman, A., Arifin, M. A. B., and Ahmed, S. (2021). A review on chitosan and chitosan-based bionanocomposites: Promising material for combatting global issues and its applications. *Int. J. Biol. Macromol.* 185, 832–848. doi:10.1016/j.ijbiomac.2021.07.023

Balakrishnan, B., Mohanty, M., Umashankar, P. R., and Jayakrishnan, A. (2005). Evaluation of an *in situ* forming hydrogel wound dressing based on oxidized alginate and gelatin. *Biomaterials* 26, 6335–6342. doi:10.1016/j.biomaterials.2005.04.012

Balan, V., Dodi, G., Mihai, C. T., Serban, A. M., and Ursachi, V. C. (2021). Biotinylated chitosan macromolecule based nanosystems: A review from chemical design to biological targets. *Int. J. Biol. Macromol.* 188, 82–93. doi:10.1016/j.ijbiomac.2021.07.197

Barros, N. R., Chen, Y., Hosseini, V., Wang, W., Nasiri, R., Mahmoodi, M., et al. (2021). Recent developments in mussel-inspired materials for biomedical applications. *Biomater. Sci.* 9, 6653–6672. doi:10.1039/d1bm01126j

Batsuli, G., and Kouides, P. (2021). Rare coagulation factor deficiencies (factors VII, X, V, and II). *Hematology/oncology Clin. N. Am.* 35, 1181–1196. doi:10.1016/j.hoc.2021.07.010

Behrens, A. M., Sikorski, M. J., and Kofinas, P. (2014). Hemostatic strategies for traumatic and surgical bleeding. *J. Biomed. Mat. Res. A* 102, 4182–4194. doi:10.1002/jbm.a.35052

Bendas, G., and Schlesinger, M. (2022). The GPIb-IX complex on platelets: Insight into its novel physiological functions affecting immune surveillance, hepatic thrombopoietin generation, platelet clearance and its relevance for cancer development and metastasis. *Exp. Hematol. Oncol.* 11, 19. doi:10.1186/s40164-022-00273-2

Benesch, J., and Tengvall, P. (2002). Blood protein adsorption onto chitosan. *Biomaterials* 23, 2561–2568. doi:10.1016/s0142-9612(01)00391-x

Bennett, B. L., and Littlejohn, L. (2014). Review of new topical hemostatic dressings for combat casualty care. *Mil. Med.* 179, 497–514. doi:10.7205/milmed-d-13-00199

Bi, S., Bao, Z., Bai, X., Hu, S., Cheng, X., and Chen, X. (2017). Tough chitosan hydrogel based on purified regeneration and alkaline solvent as biomaterials for tissue engineering applications. *Int. J. Biol. Macromol.* 104, 224–231. doi:10.1016/j.ijbiomac.2017.06.017

Biranje, S. S., Madiwale, P. V., Patankar, K. C., Chhabra, R., Bangde, P., Dandekar, P., et al. (2020). Cytotoxicity and hemostatic activity of chitosan/carrageenan composite wound healing dressing for traumatic hemorrhage. *Carbohydr. Polym.* 239, 116106. doi:10.1016/j.carbpol.2020.116106

Blair, S. D., Backhouse, C. M., Harper, R., Matthews, J., and McCollum, C. N. (1988). Comparison of absorbable materials for surgical haemostasis. *Br. J. Surg.* 75, 969–971. doi:10.1002/bjs.1800751010

Briete, L. D., Towers, W. F., Bone, R., Nair, R., Steck, M., Cutshall, B. T., et al. (2022). Perioperative anticoagulation management. *Crit. Care Nurs. Q.* 45, 119–131. doi:10.1097/cnq.0000000000000395

Broos, K., Feys, H. B., De Meyer, S. F., Vanhoorelbeke, K., and Deckmyn, H. (2011). Platelets at work in primary hemostasis. *Blood Rev.* 25, 155–167. doi:10.1016/j.blre.2011.03.002

Camire, R. M. (2021). Blood coagulation factor X: Molecular biology, inherited disease, and engineered therapeutics. *J. Thromb. Thrombolysis* 52, 383–390. doi:10.1007/s11239-021-02456-w

Cao, J., Xiao, L., and Shi, X. (2019). Injectable drug-loaded polysaccharide hybrid hydrogels for hemostasis. *RSC Adv.* 9, 36858–36866. doi:10.1039/c9ra07116d

Caprifico, A. E., Foot, P. J. S., Polycarpou, E., and Calabrese, G. (2021). Overcoming the protein corona in chitosan-based nanoparticles. *Drug Discov. Today* 26, 1825–1840. doi:10.1016/j.drudis.2021.04.014

Chen, H., Lan, G., Ran, L., Xiao, Y., Yu, K., Lu, B., et al. (2018). A novel wound dressing based on a Konjac glucomannan/silver nanoparticle composite sponge effectively kills bacteria and accelerates wound healing. *Carbohydr. Polym.* 183, 70–80. doi:10.1016/j.carbpol.2017.11.029

Chou, T.-C., Fu, E., Wu, C.-J., and Yeh, J.-H. (2003). Chitosan enhances platelet adhesion and aggregation. *Biochem. Biophysical Res. Commun.* 302, 480–483. doi:10.1016/s0006-291x(03)00173-6

Chouhan, D., and Mandal, B. B. (2020). Silk biomaterials in wound healing and skin regeneration therapeutics: From bench to bedside. *Acta biomater.* 103, 24–51. doi:10.1016/j.actbio.2019.11.050

Chung, Y. J., An, S. Y., Yeon, J. Y., Shim, W. S., and Mo, J. H. (2016). Effect of a chitosan gel on hemostasis and prevention of adhesion after endoscopic sinus surgery. *Clin. Exp. Otorhinolaryngol.* 9, 143–149. doi:10.21053/ceo.2015.00591

Colomina, M. J., Contreras, L., Guilabert, P., Koo, M., Méndez, E., and Sabate, A. (2021). Clinical use of tranexamic acid: Evidences and controversies. *Braz. J. Anesthesiol.* S0104-0014 (21), 00369–9. doi:10.1016/j.bjane.2021.08.022

Croisier, F., and Jérôme, C. (2013). Chitosan-based biomaterials for tissue engineering. *Eur. Polym. J.* 49, 780–792. doi:10.1016/j.eurpolymj.2012.12.009

Davis, S., Nawab, A., van Nispen, C., and Pourmand, A. (2021). The role of tranexamic acid in the management of an acutely hemorrhaging patient. *Hosp. Pharm.* 56, 350–358. doi:10.1177/0018578720906613

Deineka, V., Sulaieva, O., Pernakov, M., Korniienko, V., Husak, Y., Yanovska, A., et al. (2021). Hemostatic and tissue regeneration performance of novel electrospun chitosan-based materials. *Biomedicines* 9, 588. doi:10.3390/biomedicines9060588

Ding, J., Zhang, J., Li, J., Li, D., Xiao, C., Xiao, H., et al. (2019). Electrospun polymer biomaterials. *Prog. Polym. Sci.* 90, 1–34. doi:10.1016/j.progpolymsci.2019.01.002

Durand, M. J., and Gutterman, D. D. (2013). Diversity in mechanisms of endothelium-dependent vasodilation in health and disease. *Microcirculation* 20, 239–247. doi:10.1111/micc.12040

Eden, C., Buonomo, O. C., Busch, J., Gilabert-Estelles, J., Medrano, R., Nosotti, M., et al. (2021). An international multidisciplinary peer-driven consensus on the optimal use of hemostatic powders in surgical practice. *Updat. Surg.* 73, 1267–1273. doi:10.1007/s13304-021-01136-x

Elçin, A. E., Elçin, Y. M., and Elcin, Y. M. (2020). Macroporous elastic cryogels based on platelet lysate and oxidized dextran as tissue engineering scaffold: *In vitro* and *in vivo* evaluations. *Mater. Sci. Eng. C* 110, 110703. doi:10.1016/j.msec.2020.110703

Fan, X., Li, M., Yang, Q., Wan, G., Li, Y., Li, N., et al. (2021). Morphology-controllable cellulose/chitosan sponge for deep wound hemostasis with surfactant and pore-foaming agent. *Mater. Sci. Eng. C* 118, 111408. doi:10.1016/j.msec.2020.111408

Fan, X., Li, Y., Li, N., Wan, G., Ali, M. A., and Tang, K. (2020). Rapid hemostatic chitosan/cellulose composite sponge by alkali/urea method for massive haemorrhage. *Int. J. Biol. Macromol.* 164, 2769–2778. doi:10.1016/j.ijbiomac.2020.07.312

Fathi, P., Sikorski, M., Christodoulides, K., Langan, K., Choi, Y. S., Titcomb, M., et al. (2018). Zeolite-loaded alginate-chitosan hydrogel beads as a topical hemostat. *J. Biomed. Mat. Res.* 106, 1662–1671. doi:10.1002/jbm.b.33969

Feng, C., Li, J., Wu, G. S., Mu, Y. Z., Kong, M., Jiang, C. Q., et al. (2016). Chitosan-coated diatom silica as hemostatic agent for hemorrhage control. *ACS Appl. Mat. Interfaces* 8, 34234–34243. doi:10.1021/acsami.6b12317

Feng, Y. H., Zhang, S. W., and Shi, J. Y. (2020). Dpddi: A deep predictor for drug-drug interactions. *BMC Bioinforma.* 21, 419. doi:10.1186/s12859-020-03724-x

Gioutsos, K., Nguyen, T. L., Biber, U., Enderle, M. D., Koss, A., and Kocher, G. J. (2022). Surgical smoke: Modern mobile smoke evacuation systems improve occupational safety in the operating theatre. *Interact. Cardiovasc. Thorac. Surg.* 34, 775–782. doi:10.1093/icvts/ivac024

Granville-Chapman, J., Jacobs, N., and Midwinter, M. J. (2011). Pre-hospital haemostatic dressings: A systematic review. *Injury* 42, 447–459. doi:10.1016/j.injury.2010.09.037

Hafsa, J., Smach, M. A., Mrid, R. B., Sobeh, M., Majdoub, H., and Yasri, A. (2021). Functional properties of chitosan derivatives obtained through maillard reaction: A novel promising food preservative. *Food Chem.* 349, 129072. doi:10.1016/j.foodchem.2021.129072

Hao, R., Peng, X., Zhang, Y., Chen, J., Wang, T., Wang, W., et al. (2020). Rapid hemostasis resulting from the synergism of self-assembling short peptide and O-carboxymethyl chitosan. *ACS Appl. Mat. Interfaces* 12, 55574–55583. doi:10.1021/acsami.0c15480

He, Q., Gong, K., Ao, Q., Ma, T., Yan, Y., Gong, Y., et al. (2011). Positive charge of chitosan retards blood coagulation on chitosan films. *J. Biomater. Appl.* 27, 1032–1045. doi:10.1177/0885328211432487

He, W., Huang, X., Zhang, J., Zhu, Y., Liu, Y., Liu, B., et al. (2021). CaCO(3)-Chitosan composites granules for instant hemostasis and wound healing. *Mater. (Basel)* 14, 3350. doi:10.3390/ma14123350

Herrold, J. A., Adnan, S., Romagnoli, A., Madurska, M. J., Betzold, R., DuBose, J., et al. (2021). Certification in endovascular hemostasis for trauma surgeons: Possible and practical? *J. Trauma Acute Care Surg.* 91, 1.

Howe, N., and Cherpelis, B. (2013). Obtaining rapid and effective hemostasis: Part I. Update and review of topical hemostatic agents. *J. Am. Acad. Dermatology* 69, 659.e1–659.e17. doi:10.1016/j.jaad.2013.07.014

Hu, Z., Zhang, D. Y., Lu, S. T., Li, P. W., and Li, S. D. (2018). Chitosan-based composite materials for prospective hemostatic applications. *Mar. drugs* 16, 273. doi:10.3390/md16080273

Huang, N., Lin, J., Li, S., Deng, Y., Kong, S., Hong, P., et al. (2018). Preparation and evaluation of squid ink polysaccharide-chitosan as a wound-healing sponge. *Mater. Sci. Eng. C* 82, 354–362. doi:10.1016/j.msec.2017.08.068

Huerta-Madroñal, M., Caro-León, J., Espinosa-Cano, E., Aguilar, M. R., and Vázquez-Lasa, B. (2021). Chitosan - rosmarinic acid conjugates with antioxidant, anti-inflammatory and photoprotective properties. *Carbohydr. Polym.* 273, 118619. doi:10.1016/j.carbpol.2021.118619

Jing, H., and Fang, W. (2018). Effect of cationicity of carboxymethyl chitosan hydrogels on haemostatic activities and its haemostatic mechanism. *China Sci.* 13, 1325–1328.

Kalsoom Khan, A., Saba, A. U., Nawazish, S., Akhtar, F., Rashid, R., Mir, S., et al. (2017). Carrageenan based bionanocomposites as drug delivery tool with special emphasis on the influence of ferromagnetic nanoparticles. *Oxidative Med. Cell. Longev.* 2017, 1–13. doi:10.1155/2017/8158315

Kamath, K., Kamath, S. U., and Tejaswi, P. (2021). Incidence and factors influencing tourniquet pain. *Chin. J. Traumatology* 24, 291–294. doi:10.1016/j.cjtee.2021.05.002

Kandra, P., Challa, M. M., and Kalangi Padma Jyothi, H. (2012). Efficient use of shrimp waste: Present and future trends. *Appl. Microbiol. Biotechnol.* 93, 17–29. doi:10.1007/s00253-011-3651-2

Khan, M. A., and Mujahid, M. (2019). A review on recent advances in chitosan based composite for hemostatic dressings. *Int. J. Biol. Macromol.* 124, 138–147. doi:10.1016/j.ijbiomac.2018.11.045

Koumentakou, I., Terzopoulou, Z., Michopoulou, A., Kalafatakis, I., Theodorakis, K., Tzetzis, D., et al. (2020). Chitosan dressings containing inorganic additives and levofloxacin as potential wound care products with enhanced hemostatic properties. *Int. J. Biol. Macromol.* 162, 693–703. doi:10.1016/j.ijbiomac.2020.06.187

Lam, W., and Moosavi, L. (2022). *Physiology, factor V, StatPearls*. Treasure Island (FL): StatPearls Publishing LLC.

Lan, G., Lu, B., Wang, T., Wang, L., Chen, J., Yu, K., et al. (2015). Chitosan/gelatin composite sponge is an absorbable surgical hemostatic agent. *Colloids Surfaces B Biointerfaces* 136, 1026–1034. doi:10.1016/j.colsurfb.2015.10.039

Lee, Y.-H., and Lin, S.-J. (2022). Chitosan/PVA hetero-composite hydrogel containing antimicrobials, perfluorocarbon nanoemulsions, and growth factor-loaded nanoparticles as a multifunctional dressing for diabetic wound healing: Synthesis, characterization, and *in vitro/in vivo* evaluation. *Pharmaceutics* 14, 537. doi:10.3390/pharmaceutics14030537

Li, B., Wang, J., Gui, Q., and Yang, H. (2020). Continuous production of uniform chitosan beads as hemostatic dressings by a facile flow injection method. *J. Mat. Chem. B* 8, 7941–7946. doi:10.1039/d0tb01462a

Li, H., Zhou, X., Luo, L., Ding, Q., and Tang, S. (2022). Bio-orthogonally crosslinked catechol–chitosan hydrogel for effective hemostasis and wound healing. *Carbohydr. Polym.* 281, 119039. doi:10.1016/j.carbpol.2021.119039

Li, J., Cao, W., Lv, X. X., Jiang, L., Li, Y. J., Li, W. Z., et al. (2013). Zeolite-based hemostat QuikClot releases calcium into blood and promotes blood coagulation *in vitro*. *Acta Pharmacol. Sin.* 34, 367–372. doi:10.1038/aps.2012.159

Li, J., Sun, X., Zhang, K., Yang, G., Mu, Y., Su, C., et al. (2020). Chitosan/diatom-biosilica aerogel with controlled porous structure for rapid hemostasis. *Adv. Healthc. Mat.* 9, 2000951. doi:10.1002/adhm.202000951

Li, X., Xing, R., Xu, C., Liu, S., Qin, Y., Li, K., et al. (2021). Immunostimulatory effect of chitosan and quaternary chitosan: A review of potential vaccine adjuvants. *Carbohydr. Polym.* 264, 118050. doi:10.1016/j.carbpol.2021.118050

Liang, Y., Chen, B., Li, M., He, J., Yin, Z., and Guo, B. (2020). Injectable Antimicrobial conductive hydrogels for wound disinfection and infectious wound healing. *Biomacromolecules* 21, 1841–1852. doi:10.1021/acs.biomac.9b01732

Lim, Y.-S., Ok, Y.-J., Hwang, S.-Y., Kwak, J.-Y., and Yoon, S. (2019). Marine collagen as A promising biomaterial for biomedical applications. *Mar. drugs* 17, 467. doi:10.3390/md17080467

Lin, Y. T., Hsieh, C. J., and Lee, L. Y. (2021). The efficacy of chitosan hemostatic pad on hemostatic function in patients undergoing cardiac catheterization: A systematic review and meta-analysis. *Heart Surg. Forum* 24, E833–e841. doi:10.1532/hsf.3997

Liu, W., Yang, C., Gao, R., Zhang, C., Ou-Yang, W., Feng, Z., et al. (2021). Polymer composite sponges with inherent antibacterial, hemostatic, inflammation-modulating and proregenerative performances for methicillin-resistant Staphylococcus aureus-infected wound healing. *Adv. Healthc. Mat.* 10, e2101247. doi:10.1002/adhm.202101247

Long, M., Zhang, Y., Huang, P., Chang, S., Hu, Y., Yang, Q., et al. (2018). Nanoclay haemostatics: Emerging nanoclay composite for effective hemostasis (adv. Funct. Mater. 10/2018). *Adv. Funct. Mat.* 28, 1870062. doi:10.1002/adfm.201870062

Maier Greg, P., Rapp Michael, V., Waite, J. H., Israelachvili Jacob, N., and Butler, A. (2015). Adaptive synergy between catechol and lysine promotes wet adhesion by surface salt displacement. *Science* 349, 628–632. doi:10.1126/science.aab0556

Malda, J., Kreijveld, E., Temenoff, J. S., Blitterswijk, C. A. v., and Riesle, J. (2003). Expansion of human nasal chondrocytes on macroporous microcarriers enhances redifferentiation. *Biomaterials* 24, 5153–5161. doi:10.1016/s0142-9612(03)00428-9

Méndez-Barbero, N., Gutiérrez-Muñoz, C., and Blanco-Colio, L. M. (2021). Cellular crosstalk between endothelial and smooth muscle cells in vascular wall remodeling. *Int. J. Mol. Sci.* 22, 7284. doi:10.3390/ijms22147284

Merajikhah, A., Imani, B., Khazaei, S., and Bouraghi, H. (2022). Impact of surgical smoke on the surgical team and operating room nurses and its reduction strategies: A systematic review. *Iran. J. Public Health* 51, 27–36. doi:10.18502/ijph.v51i1.8289

Michels, A., Lillicrap, D., and Yacob, M. (2022). Role of von Willebrand factor in venous thromboembolic disease. *JVS-vascular Sci.* 3, 17–29. doi:10.1016/j.jvssci.2021.08.002

Millner, R., Lockhart, A. S., and Marr, R. (2010). Chitosan arrests bleeding in major hepatic injuries with clotting dysfunction: An *in vivo* experimental study in a model of hepatic injury in the presence of moderate systemic heparinisation. *annals* 92, 559–561. doi:10.1308/003588410x12699663903593

Neubauer, K., and Zieger, B. (2022). Endothelial cells and coagulation. *Cell Tissue Res.* 387, 391–398. doi:10.1007/s00441-021-03471-2

Okuda-Tanino, A., Sugawara, D., Tashiro, T., Iwashita, M., Obara, Y., Moriya, T., et al. (2017). Licochalcones extracted from Glycyrrhiza inflata inhibit platelet aggregation accompanied by inhibition of COX-1 activity. *PloS one* 12, e0173628. doi:10.1371/journal.pone.0173628

Othman, S. I., Alturki, A. M., Abu-Taweel, G. M., Altoom, N. G., Allam, A. A., and Abdelmonem, R. (2021). Chitosan for biomedical applications, promising antidiabetic drug delivery system, and new diabetes mellitus treatment based on stem cell. *Int. J. Biol. Macromol.* 190, 417–432. doi:10.1016/j.ijbiomac.2021.08.154

Pai, M. (2021). Acquired hemophilia A. *Hematology/oncology Clin. N. Am.* 35, 1131–1142. doi:10.1016/j.hoc.2021.07.007

Pan, M., Tang, Z., Tu, J., Wang, Z., Chen, Q., Xiao, R., et al. (2018). Porous chitosan microspheres containing zinc ion for enhanced thrombosis and hemostasis. *Mater. Sci. Eng. C* 85, 27–36. doi:10.1016/j.msec.2017.12.015

Paquette, I. M., Madoff, R. D., Sigurdson, E. R., and Chang, G. J. (2018). Impact of proximal vascular ligation on survival of patients with colon cancer. *Ann. Surg. Oncol.* 25, 38–45. doi:10.1245/s10434-016-5720-3

Rao, K. M., Narayanan, K. B., Uthappa, U. T., Park, P. H., Choi, I., and Han, S. S. (2022). Tissue adhesive, self-healing, biocompatible, hemostasis, and antibacterial properties of fungal-derived carboxymethyl chitosan-polydopamine hydrogels. *Pharmaceutics* 14, 1028. doi:10.3390/pharmaceutics14051028

Rasool, A., Ata, S., and Islam, A. (2019). Stimuli responsive biopolymer (chitosan) based blend hydrogels for wound healing application. *Carbohydr. Polym.* 203, 423–429. doi:10.1016/j.carbpol.2018.09.083

Ren, Y., Sun, X., Chen, L., Li, Y., Sun, M., Duan, X., et al. (2021). Structures and impact strength variation of chemically crosslinked high-density polyethylene: Effect of crosslinking density. *RSC Adv.* 11, 6791–6797. doi:10.1039/d0ra10365a

Roshkovan, L., Singhal, S., Katz, S. I., and Galperin-Aizenberg, M. (2021). Multimodality imaging of Surgicel(®), an important mimic of post-operative complication in the thorax. *BJR Open* 3, 20210031. doi:10.1259/bjro.20210031

Ruggeri, Z. M., and von Willebrand factor (1997). *J. Clin. Invest.* 100, S41–S46.

Seidi, F., Khodadadi Yazdi, M., Jouyandeh, M., Dominic, M., Naeim, H., Nezhad, M. N., et al. (2021). Chitosan-based blends for biomedical applications. *Int. J. Biol. Macromol.* 183, 1818–1850. doi:10.1016/j.ijbiomac.2021.05.003

Shah, S., and da Cruz, M. J. (2021). Composite gelfoam/fascia graft: A novel technique in tympanoplasty surgery. *Eur. Arch. Otorhinolaryngol.* 278, 4605–4606. doi:10.1007/s00405-021-07042-7

Shariatinia, Z. (2018). Carboxymethyl chitosan: Properties and biomedical applications. *Int. J. Biol. Macromol.* 120, 1406–1419. doi:10.1016/j.ijbiomac.2018.09.131

Shi, Z., Lan, G., Hu, E., Lu, F., Qian, P., Liu, J., et al. (2020). Puff pastry-like chitosan/konjac glucomannan matrix with thrombin-occupied microporous starch particles as a composite for hemostasis. *Carbohydr. Polym.* 232, 115814. doi:10.1016/j.carbpol.2019.115814

Shou, Y., Zhang, J., Yan, S., Xia, P., Xu, P., Li, G., et al. (2020). Thermoresponsive chitosan/DOPA-based hydrogel as an injectable therapy approach for tissue-adhesion and hemostasis. *ACS Biomater. Sci. Eng.* 6, 3619–3629. doi:10.1021/acsbiomaterials.0c00545

Sirotkina, O. V., Laskovets, A. B., Andoskin, P. A., Emelyanov, A. K., Zabotina, A. M., and Vavilova, T. V. (2016). Increase in GP IIb-IIIa and P2Y12 Receptors in Activated Platelets as the Possible Indicator of de novo Protein Synthesis. *Mol. Biol. Los. Angel.* 50, 111–117. doi:10.1134/s0026893316010180

Slowing, I. I., Wu, C.-W., Vivero-Escoto, J. L., and Lin, V. S. Y. (2009). Mesoporous silica nanoparticles for reducing hemolytic activity towards mammalian red blood cells. *Small* 5, 57–62. doi:10.1002/smll.200800926

Sokolakis, I., Pyrgidis, N., and Hatzichristodoulou, G. (2022). The use of collagen fleece (TachoSil) as grafting material in the surgical treatment of Peyronie's disease. A comprehensive narrative review. *Int. J. Impot. Res.* 34, 260–268. doi:10.1038/s41443-020-00401-8

Song, F., Kong, Y., Shao, C., Cheng, Y., Lu, J., Tao, Y., et al. (2021). Chitosan-based multifunctional flexible hemostatic bio-hydrogel. *Acta biomater.* 136, 170–183. doi:10.1016/j.actbio.2021.09.056

Sukhinina, T. S., Pevzner, D. V., Mazurov, A. V., Vlasik, T. N., Solovieva, N. G., Kostritca, N. S., et al. (2022). The role of platelet glycoprotein IIb/IIIa inhibitors in current treatment of acute coronary syndrome. *Kardiologiia* 62, 64–72. doi:10.18087/cardio.2022.4.n2020

Sun, S., Urbanus, R. T., Ten Cate, H., de Groot, P. G., de Laat, B., Heemskerk, J. W. M., et al. (2021). Platelet activation mechanisms and consequences of immune thrombocytopenia. *Cells* 10, 3386. doi:10.3390/cells10123386

Tefik, T., Sanli, O., Oktar, T., Yucel, O. B., Ozluk, Y., and Kilicaslan, I. (2012). Oxidized regenerated cellulose granuloma mimicking recurrent mass lesion after laparoscopic nephron sparing surgery. *Int. J. Surg. case Rep.* 3, 227–230. doi:10.1016/j.ijscr.2012.03.001

Varshosaz, J. (2007). The promise of chitosan microspheres in drug delivery systems. *Expert Opin. drug Deliv.* 4, 263–273. doi:10.1517/17425247.4.3.263

Vu, T. T., Fredenburgh, J. C., and Weitz, J. I. (2013). Zinc: An important cofactor in haemostasis and thrombosis. *Thromb. Haemost.* 109, 421–430. doi:10.1160/th12-07-0465

Wang, C. H., Cherng, J. H., Liu, C. C., Fang, T. J., Hong, Z. J., Chang, S. J., et al. (2021). Procoagulant and antimicrobial effects of chitosan in wound healing. *Int. J. Mol. Sci.* 22, 7067. doi:10.3390/ijms22137067

Wang, X.-X., Liu, Q., Sui, J.-X., Ramakrishna, S., Yu, M., Zhou, Y., et al. (2019). Recent advances in hemostasis at the nanoscale. *Adv. Healthc. Mater.* 8, 1900823.

Wang, X., Dang, Q., Liu, C., Chang, G., Song, H., Xu, Q., et al. (2022). Antibacterial porous sponge fabricated with capric acid-grafted chitosan and oxidized dextran as a novel hemostatic dressing. *Carbohydr. Polym.* 277, 118782. doi:10.1016/j.carbpol.2021.118782

Wang, Y., Fu, Y., Li, J., Mu, Y., Zhang, X., Zhang, K., et al. (2018). Multifunctional chitosan/dopamine/diatom-biosilica composite beads for rapid blood coagulation. *Carbohydr. Polym.* 200, 6–14. doi:10.1016/j.carbpol.2018.07.065

Wang, Y. H., Liu, C. C., Cherng, J. H., Fan, G. Y., Wang, Y. W., Chang, S. J., et al. (2019). Evaluation of chitosan-based dressings in a swine model of artery-injury-related shock. *Sci. Rep.* 9, 14608. doi:10.1038/s41598-019-51208-7

Wang, Y. W., Liu, C. C., Cherng, J. H., Lin, C. S., Chang, S. J., Hong, Z. J., et al. (2019). Biological effects of chitosan-based dressing on hemostasis mechanism. *Polym. (Basel)* 11, 1906. doi:10.3390/polym11111906

Wang, Z., Ke, M., He, L., Dong, Q., Liang, X., Rao, J., et al. (2021). Biocompatible and antibacterial soy protein isolate/quaternized chitosan composite sponges for acute upper gastrointestinal hemostasis. *Regen. Biomater.* 8, rbab034. doi:10.1093/rb/rbab034

Watters, D. A., Foran, P., McKinley, S., and Campbell, G. (2022). Clearing the air on surgical plume. *ANZ J. Surg.* 92, 57–61. doi:10.1111/ans.17340

Wu, J., Zhang, L., Wang, Y., Long, Y., Gao, H., Zhang, X., et al. (2011). Mussel-Inspired chemistry for robust and surface-modifiable multilayer films. *Langmuir* 27, 13684–13691. doi:10.1021/la2027237

Wu, X., Tang, Z., Liao, X., Wang, Z., and Liu, H. (2020). Fabrication of chitosan@ calcium alginate microspheres with porous core and compact shell, and application as a quick traumatic hemostat. *Carbohydr. Polym.* 247, 116669. doi:10.1016/j.carbpol.2020.116669

Xia, L., Wang, S., Jiang, Z., Chi, J., Yu, S., Li, H., et al. (2021). Hemostatic performance of chitosan-based hydrogel and its study on biodistribution and biodegradability in rats. *Carbohydr. Polym.* 264, 117965. doi:10.1016/j.carbpol.2021.117965

Yadav, L. R., Chandran, S. V., Lavanya, K., and Selvamurugan, N. (2021). Chitosan-based 3D-printed scaffolds for bone tissue engineering. *Int. J. Biol. Macromol.* 183, 1925–1938. doi:10.1016/j.ijbiomac.2021.05.215

Yan, D., Li, Y., Liu, Y., Li, N., Zhang, X., and Yan, C. (2021). Antimicrobial properties of chitosan and chitosan derivatives in the treatment of enteric infections. *Molecules* 26, 7136. doi:10.3390/molecules26237136

Yang, E., Hou, W., Liu, K., Yang, H., Wei, W., Kang, H., et al. (2022). A multifunctional chitosan hydrogel dressing for liver hemostasis and infected wound healing. *Carbohydr. Polym.* 291, 119631. doi:10.1016/j.carbpol.2022.119631

Yang, J., Tian, F., Wang, Z., Wang, Q., Zeng, Y. J., and Chen, S. Q. (2008). Effect of chitosan molecular weight and deacetylation degree on hemostasis. *J. Biomed. Mat. Res.* 84, 131–137. doi:10.1002/jbm.b.30853

Yang, M., Li, J., Gu, P., and Fan, X. (2021). The application of nanoparticles in cancer immunotherapy: Targeting tumor microenvironment. *Bioact. Mater.* 6, 1973–1987. doi:10.1016/j.bioactmat.2020.12.010

Younes, I., and Rinaudo, M. (2015). Chitin and chitosan preparation from marine sources. Structure, properties and applications. *Mar. drugs* 13, 1133–1174. doi:10.3390/md13031133

Yuan, H., Chen, L., and Hong, F. F. (2020). A biodegradable antibacterial nanocomposite based on oxidized bacterial nanocellulose for rapid hemostasis and wound healing. *ACS Appl. Mat. Interfaces* 12, 3382–3392. doi:10.1021/acsami.9b17732

Zanchetta, F. C., Trinca, R. B., Gomes Silva, J. L., Breder, J. D., Cantarutti, T. A., Consonni, S. R., et al. (2020). Effects of electrospun fibrous membranes of PolyCaprolactone and chitosan/poly(ethylene oxide) on mouse acute skin lesions. *Polym. (Basel)* 12, 1580. doi:10.3390/polym12071580

Zhang, M., Wang, D., Ji, N., Lee, S., Wang, G., Zheng, Y., et al. (2021). Bioinspired design of sericin/chitosan/Ag@MOF/GO hydrogels for efficiently combating resistant bacteria, rapid hemostasis, and wound healing. *Polym. (Basel)* 13, 2812. doi:10.3390/polym13162812

Zhang, X., Sun, G.-h., Tian, M.-p., Wang, Y.-n., Qu, C.-c., Cheng, X.-j., et al. (2019). Mussel-inspired antibacterial polydopamine/chitosan/temperature-responsive hydrogels for rapid hemostasis. *Int. J. Biol. Macromol.* 138, 321–333. doi:10.1016/j.ijbiomac.2019.07.052

Zhao, W.-Y., Fang, Q.-Q., Wang, X.-F., Wang, X.-W., Zhang, T., Shi, B.-H., et al. (2020). Chitosan-calcium alginate dressing promotes wound healing: A preliminary study. *Wound Repair Regen.* 28, 326–337. doi:10.1111/wrr.12789

Zhao, X., Li, P., Guo, B., and Ma, P. X. (2015). Antibacterial and conductive injectable hydrogels based on quaternized chitosan-graft-polyaniline/oxidized dextran for tissue engineering. *Acta biomater.* 26, 236–248. doi:10.1016/j.actbio.2015.08.006

Zhao, X., Wu, H., Guo, B., Dong, R., Qiu, Y., and Ma, P. X. (2017). Antibacterial anti-oxidant electroactive injectable hydrogel as self-healing wound dressing with hemostasis and adhesiveness for cutaneous wound healing. *Biomaterials* 122, 34–47. doi:10.1016/j.biomaterials.2017.01.011

Zhao, Y. F., Zhao, J. Y., Hu, W. Z., Ma, K., Chao, Y., Sun, P. J., et al. (2019). Synthetic poly(vinyl alcohol)-chitosan as a new type of highly efficient hemostatic sponge with blood-triggered swelling and high biocompatibility. *J. Mat. Chem. B* 7, 1855–1866. doi:10.1039/c8tb03181a

Zhao, Y., Xiao, A., Wu, P., Chen, F., Zhang, Q., Liang, X., et al. (2020). Fabrication of hydroxypropyl chitosan/soy protein isolate hydrogel for effective hemorrhage control. *Tissue Eng. Part A* 27, 788–795. doi:10.1089/ten.tea.2020.0174